

GENERAL RESEARCH LIBRARY
DOCUMENT COLLECTION



OAK RIDGE NATIONAL LABORATORY

operated by

UNION CARBIDE CORPORATION

for the

U.S. ATOMIC ENERGY COMMISSION



ORNL - TM - 49

3

WASTE TREATMENT AND DISPOSAL PROGRESS REPORT
FOR AUGUST AND SEPTEMBER 1961

**CENTRAL RESEARCH LIBRARY
DOCUMENT COLLECTION
LIBRARY LOAN COPY**
DO NOT TRANSFER TO ANOTHER PERSON
If you wish someone else to see this
document, send in name with document
and the library will arrange a loan.

NOTICE

This document contains information of a preliminary nature and was prepared primarily for internal use at the Oak Ridge National Laboratory. It is subject to revision or correction and therefore does not represent a final report. The information is not to be abstracted, reprinted or otherwise given public dissemination without the approval of the ORNL patent branch, Legal and Information Control Department.

LEGAL NOTICE

This report was prepared as an account of Government sponsored work. Neither the United States, nor the Commission, nor any person acting on behalf of the Commission:

- A. Makes any warranty or representation, expressed or implied, with respect to the accuracy, completeness, or usefulness of the information contained in this report, or that the use of any information, apparatus, method, or process disclosed in this report may not infringe privately owned rights; or
- B. Assumes any liabilities with respect to the use of, or for damages resulting from the use of any information, apparatus, method, or process disclosed in this report.

As used in the above, "person acting on behalf of the Commission" includes any employee or contractor of the Commission, or employee of such contractor, to the extent that such employee or contractor of the Commission, or employee of such contractor prepares, disseminates, or provides access to, any information pursuant to his employment or contract with the Commission, or his employment with such contractor.

CHEMICAL TECHNOLOGY DIVISION
AND
HEALTH PHYSICS DIVISION

WASTE TREATMENT AND DISPOSAL PROGRESS REPORT
FOR AUGUST AND SEPTEMBER 1961

R. E. Blanco and E. G. Struxness

DATE ISSUED

NOV 29 1961

OAK RIDGE NATIONAL LABORATORY
Oak Ridge, Tennessee
operated by
UNION CARBIDE CORPORATION
for the
U.S. ATOMIC ENERGY COMMISSION



3 4456 0049727 3

ABSTRACT

High-Level Waste Calcination. Nine calcination runs were completed in the engineering-scale equipment, 8-in.-dia by 90-in.-high stainless steel calcination pots. Both batch and continuous evaporators were used in processing simulated Purex and TBP-25 wastes prior to calcination. Calciner feed rates averaged 25-31 liters/hr when the pots were filled to 90% of capacity. In two runs where organic phosphates were present, average feed rates were less by a factor of 4 because of excessive foaming in the calciner.

Waste oxide from TBP-25 waste was incorporated into glassy materials at 875-1000°C by the addition of phosphate with borate and lead oxide fluxing agents. The solids had densities of 2.36 to 2.84 g/ml and represented waste volume reduction factors of 7.2-8.4. The condensates from batch evaporations of TBP-25 waste made 2 M in sodium hypophosphite contained 0.48 and 0.71% of the original ruthenium. The condensates contained less ruthenium when these feeds were made 0.25 M in PbO than when 0.25 M in $Pb(NO_3)_2$ (0.68 vs 2.18%). The principal gaseous product from the reaction between iron or aluminum nitrate (1-2 M) and phosphorous acid (1 M) appears to be nitric oxide. The best catalysts found for the reaction between nitrate and phosphite ions were silver, mercuric, and palladium ions. Vapor-liquid equilibrium conditions were investigated for simulated TBP-25, Darex, and Purex waste solutions as a function of acid and salt concentrations. Densities of the solutions were measured as a function of temperature and pressure.

A 4-in.-dia by 24-in.-high stainless steel pot calciner and related equipment for use with actual wastes in a hot cell is being designed. This equipment will be used primarily to study fission product volatility during evaporation and calcination, but will also provide solids that can be studied for radiation stability and analyzed for fission product distribution.

Preparation of chemical flowsheets for the pot calcination pilot plant at ICPP was started, with the initial objective of sizing process equipment to handle the maximum flows to be expected. The original process flowsheet was changed to delete the gas holder and recycle equipment and to provide for absorption of excess NO_2 in the acid scrubber. Design of mechanical equipment for demonstration of the pot calciner positioning, connecting, and sealing procedures is ~60% complete.

Low-Level Waste Treatment. The last demonstration run on process waste water in the semi-pilot plant facility gave effluent with <10% of the MPC for >1500 bed volumes of waste treated. Total hardness in the clarifier overflow averaged 20 ppm. The early breakthrough in an earlier run is believed to have been due to carbonate deficiency in the feed, which resulted in saturation of the resin with calcium. This will be forestalled in the pilot plant by continuous analysis of the effluent for hardness.

Installation of the 10-gpm low-activity waste pilot plant is complete, including an enclosed type 3 FLC Oliver vacuum filter substituted for an

Eimco-Burwell plate-and-frame filter to concentrate the sludge effluent from the clarifier. Approximately 300 hr of nonradioactive processing was accomplished with ORNL tap water, with the objectives of orienting personnel, optimizing operating procedures, and testing equipment. Tests by Dorr-Oliver, Inc., to classify solids in the treatment plant effluent showed that the suspended solids contained 59% of the Cs-137 and that the percentage of non-CaCO₃ solids increased as the particle size of the solids decreased; these results suggested the need for improving both the sorptive and the settling properties of Grundite (illite). In laboratory tests, heat-treatment of Grundite increased removal (from 83 to 96%) of Cs-137 from ORNL process waste water. Heat treatment to 600°C increased the selectivity of Grundite for cesium and decreased the percentage of small particle sizes, thus improving its settleability.

Engineering, Economic, and Hazards Evaluation. The economics of high-activity waste disposal in salt by (1) liquids in rooms with recessed floors, (2) pot calcination vessels in racks above the floor, and (3) pot calcination vessels in holes in the floor is being studied. In order to determine the amount of mine space that will be required, the infinite-slab heat calculation was used for cases 1 and 2. Gross mine area requirements for case 1 varied from 67 to 10 acres/year for decay times of 0.33 to 30 years. An equation for case 3 was programmed for the computer and the code is being "debugged."

Disposal in Deep Wells. An advisory committee to the AEC has considered several of the major problem areas encountered in the disposal of radioactive liquids to deep permeable formations and made recommendations for distributing work efforts so that the maximum utilization of the competence, facilities, and interest of the various co-operating agencies can be realized. Although ORNL will probably become involved in several phases of the program, initial efforts will be directed primarily to establishing the sorptive properties of typical permeable formations for the critical radionuclides in low- and intermediate-level waste streams.

Negotiations with Westco Research (Fort Worth) for a Laboratory sub-contract to develop a waste-cement-clay mixture for use in the proposed ORNL Fracturing Disposal Pilot Plant were completed and a proposed sub-contract was submitted to AEC for approval.

Disposal in Natural Salt Formations. Theoretical computations of temperature profiles around an isolated line source show reasonable agreement with measured profiles around two slender cylindrical heaters in a pillar and in the floor of the Hutchinson mine. Temperature measurements in the pillar and floor show that heat transfer is essentially the same in both locations despite the presence of shale and anhydrite in the floor. Values for thermal conductivity (3.0 Btu hr⁻¹ ft⁻¹ °F⁻¹) and diffusivity (0.10 ft²/hr) computed from these measurements are in good agreement with measured values in single pure salt crystals (3.0 Btu hr⁻¹ ft⁻¹ °F⁻¹ and 0.11 ft²/hr at 40°C). Preparations are underway for additional heat flow tests with multiple heat sources in geometric array in the Hutchinson mine.

Data from plastic flow gages in a recently mined room in the Hutchinson mine indicate that maximum closure of the room will amount to about 0.4% of

the opening and that 95% of this movement will take place in approximately 5.7 years.

Clinch River Studies. Core samples of bottom sediments taken at 10 equally spaced intervals along five cross-sections, CRM 4.7, 7.6, 11.9, 15.3, and 19.2, were submitted to the U.S. Geological Survey for size distribution analyses. Results of the analyses indicate that the sediments vary in texture from silty loam to loam, and that the sizes are classed as well graded clay to the upper range of sand sizes (median diameters ranging from 20 to 39 μ). The average clay content is about 14%, and the sand content varies from 30% at the lowest cross-section to 40% at the uppermost cross-section.

Results of a dispersion test, with Au-198 as a tracer, were: (1) White Oak Creek water is uniformly dispersed in width and depth of cross-section at CRM 17.1; (2) travel time from the mouth of White Oak Creek (CRM 20.8) to Centers Ferry (CRM 4.5) is 30.2 hr; and (3) the dilution factor is approximately 5000. Flow conditions under which the test was run were 7 cfs from White Oak Creek and 8000 cfs in the Clinch River, with the level of Watts Bar Reservoir held between 740 and 741 ft above mean sea level.

Fundamental Studies of Minerals. Ion exchange sites of vermiculite and montmorillonite were saturated with the cations K, Na, Li, Ca, Al, and Ba. Ba-vermiculite and K-montmorillonite sorbed the highest amounts of cesium. On slurrying 1-g equivalents of the saturated minerals with 20 ml of 1.5 M NaNO_3 solution containing 25 mg Cs/liter, Ba-vermiculite and K-montmorillonite sorbed 2.7 times and 1.6 times more cesium, respectively, than their natural counterparts after >150 hr contact. K-montmorillonite reached equilibrium within 1 hr after contact, while Ba-vermiculite did not reach equilibrium even after 190 hr. The c-spacings were partially collapsed in both cases; however, the exchange capacity of the saturated forms remained approximately the same as that of the original minerals.

White Oak Creek Basin Study. The rate of ground water movement in the bed of former White Oak Lake was measured by the auger hole method. Tests conducted in the upper lake bed show permeability values of 0.5 and 2.6 ft/day. In the lower portion of the lake bed the rate of ground water movement ranged from 0.2 to 2.2 ft/day.

CONTENTS

	Page
1.0 INTRODUCTION	6
2.0 HIGH-LEVEL WASTE CALCINATION	7
2.1 Evaporation-Calcination	7
2.2 Fixation in Glasses	7
2.3 Properties of Waste Solutions	15
2.4 Design of Hot Cell Evaporation-Calcination Equipment	15
2.5 Design of Calcination Pilot Plant	25
3.0 LOW-LEVEL WASTE TREATMENT	25
3.1 Scavenging-Ion Exchange Process	26
3.2 Inorganic Ion Exchange of Process Waste Water Plant Effluent	26
4.0 ENGINEERING, ECONOMIC, AND HAZARDS EVALUATION	31
4.1 Liquid in Salt	32
4.2 Calcination Vessels above Floor	32
5.0 DISPOSAL IN DEEP WELLS	36
5.1 Disposal by Hydraulic Fracturing	36
5.2 Liquid Injection into Permeable Formations	37
6.0 DISPOSAL IN NATURAL SALT FORMATIONS	40
6.1 Field Tests	40
6.2 Plastic Flow Studies	41
6.3 Thermal Studies	46
7.0 CLINCH RIVER STUDY	51
7.1 Estimate of Activity in Bottom Sediments	51
7.2 Dispersion Study	51
7.3 Error in Estimate of Sediment Activity	53
8.0 FUNDAMENTAL STUDIES OF MINERALS	53
8.1 Considerations in Cesium Selectivity	53
9.0 WHITE OAK CREEK BASIN STUDY	56
10.0 REFERENCES	57

1.0 INTRODUCTION

This report is the third of a series of bimonthly reports on progress in the ORNL development program, the objective of which is to develop and demonstrate on a pilot plant scale integrated processes for treatment and ultimate disposal of radioactive wastes resulting from reactor operations and reactor fuel processing in the forthcoming nuclear power industry. The wastes of concern include those of high, intermediate, and low levels of radioactivity in liquid, solid, or gaseous states.

Principal current emphasis is on high- and low-activity liquid wastes. Under the integrated plan, low-activity wastes, consisting of very dilute salt solutions, such as cooling water and canal water, would be treated by scavenging and ion exchange processes to remove radioactive constituents and the water discharged to the environment. The retained waste solids or slurries would be combined with the high-level wastes. Alternatively, the retained solids or the untreated waste could be discharged to the environment in deep geologic formations. The high-activity wastes would be stored at their sites of origin for economic periods to allow for radioactive decay and artificial cooling.

Two methods are being investigated for permanent disposal of high-activity wastes. One approach is conversion of the liquids to solids by high-temperature "pot" calcination or fixation in the final storage container (pot) itself and storage in a permanently dry environment such as a salt mine. This is undoubtedly the safest method since complete control of radioactivity can be ensured within present technology during treatment, shipping, and storage. Another approach is disposal of the liquid directly into sealed or vented salt cavities. Research and development work is planned to determine the relative feasibility, safety, and economics of these methods, although the major effort will be placed on conversion to solids and final storage as solids.

Tank storage or high-temperature calcination of intermediate-level wastes may be unattractive because of their large volumes. Consequently, other disposal methods will be studied. One method, e.g., addition of solidifying agents prior to direct disposal into impermeable shale by hydrofracturing, is under investigation at present. Particular attention is given to the engineering design and construction of an experimental fracturing plant to dispose of ORNL intermediate-level wastes by this method if proved feasible.

Environmental research on the Clinch River, motivated by the need for safe and realistic permissible limits of waste releases, is included in this program. The objective is to obtain a detailed characterization of fission product distribution, transport, and accumulation in the physical, chemical, and biological segments of this environment.

Previous reports in this series are ORNL-CF-61-7-3 and ORNL-TM-15.

2.0 HIGH-LEVEL WASTE CALCINATION

The pot calcination process for converting high-activity-level wastes to solids is being studied on both a laboratory and engineering scale to provide design information for construction of a pilot plant. Development work has been with synthetic Purex, Darex, and TBP-25 wastes (Table 2.1) containing millicurie amounts of ruthenium but has not been demonstrated on actual high-activity-level wastes. A general flowsheet was shown previously (1).

2.1 Evaporation-Calcination (J. C. Suddath, C. W. Hancher, L. J. King)

Nine waste calcination runs (five with TBP-25 and four with Purex waste) were completed in the engineering-scale, 8 in. dia by 90 in. high, stainless steel calcination pots (Table 2.2). Six runs were made with a continuous evaporator, closely coupled to the pot, and three with feed prepared in a batch evaporator. In two of the tests with TBP-25 wastes, organic phosphates representing radiation degradation products of TBP were added.

The four Purex tests (R-43 through R-46) were routinely successful with average feed rates of 25 - 33 liters/hr. The bulk densities of the calcined solids were 1.14 - 1.55 g/cc. The quantity of water added to strip HNO_3 from the feed in the evaporator in runs R-43 and 44 was greater than necessary. A more realistic value for the water-to-feed ratio would be 4 to 5.

The first TBP-25 test (R-47) was also a routine test, the pot being about 90% filled with solids. Tests R-48 and 49 were attempts to more nearly fill the pots by extending the feeding time. It was found that 10 - 20% more solids could be added to the pot by doubling the feeding time. The solids from TBP-25 feed had bulk densities ranging from 0.52 to 0.83 g/cc and appeared to have been deposited by radial deposition (Fig. 2.1).

In Runs R-50 and R-51, di- and monobutyl phosphates were each added to the feed, 1 cc per liter of waste. This is equivalent to a phosphate concentration of ~ 0.01 M. The organics caused a serious foam problem in the calciner, which resulted in reduced rates and "burp-overs" through the off-gas line.

Additional details and results of these nine runs will be presented when analysis of the data has been completed.

2.2 Fixation in Glasses (W. E. Clark, H. W. Godbee, and K. L. Servis)

Simulated TBP-25 waste was incorporated into melts at 875-1000°C. On being cooled and either quenched or annealed, the melts gave glassy solids with densities of 2.36 to 2.84 g/ml, representing volume reduction factors from 7.2 to 8.4. One of the more satisfactory mixtures, from consideration of behavior during heating, softening point, fluidity of melt, and quality of final product, gave a glass with 40.5, 25.0, 18.6, and 15.9 wt %, respectively, P_2O_5 , Al_2O_3 , Na_2O and PbO (Table 2.3, melt 7, and Fig. 2.2).

UNCLASSIFIED
PHOTO 55670

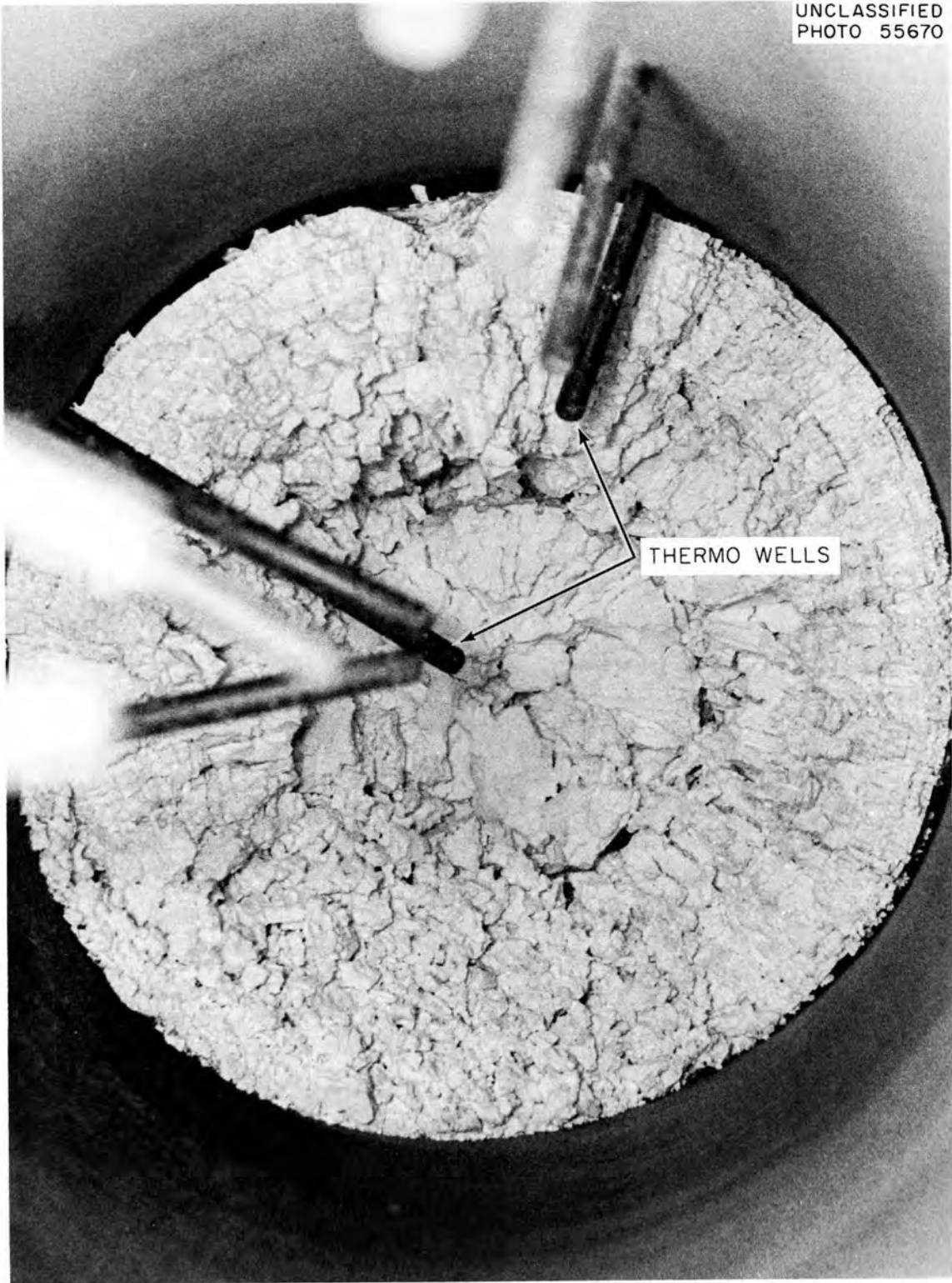


Fig. 2.1. Example of Radial Deposition of TBP-25 Calcined Solids.



Fig. 2.2. Phosphate-Lead Glass Incorporating TBP-25 Waste Oxides. Additives per liter of waste: 2.0 moles of $\text{NaH}_2\text{PO}_2 \cdot \text{H}_2\text{O}$ and 0.25 mole of PbO .

Table 2.1. Compositions of Simulated High-Activity Wastes

Component	Amount (moles/liter)		
	Purex	TBP-25	Darex
Al ³⁺	0.1	1.72	---
Fe ³⁺	0.5	0.003	1.2
Cr ³⁺	0.01	---	0.4
Ni ⁺⁺	0.01	---	0.2
Na ⁺	0.6	0.1	---
H ⁺	5.6	1.26	2.0
Hg ⁺⁺	---	0.02	---
NH ₄ ⁺	---	0.05	---
Mn ⁺⁺	---	---	0.04
NO ₃ ⁻	6.1	6.6	7.2
SO ₄ ⁼	1.0	---	---
Cl ⁻	---	---	0.001

Table 2.2. Engineering-Scale Evaporation and Pot Calcination of Wastes to 900°C

Run No.	Waste Type	Evaporator	Feed Time (hr)	Avg. Feed (liters/hr)	Calc. Time (hr)	Water/Feed Ratio	Bulk Density ^b (g/cc)
R-43	Purex	Cont.	13	31	15	9.1	1.29
R-44	Purex	Cont.	12	33	11	7.9	1.14
R-45	Purex	Batch	13	25	11	3.8	1.17
R-46	Purex	Batch	15	28	10	3.0	1.55
R-47	TBP-25	Cont.	14	31	10	4.8	0.57
R-48	TBP-25	Cont.	38	12	10	2.8	0.77
R-49	TBP-25	Cont.	27	18	10	3.6	0.83
R-50	TBP-25	Cont. ^a	33	11	8	3.3	0.52
R-51	TBP-25	Batch ^a	43	7	7	3.1	0.59

^a Organic phosphates added.

^b Weight of solid after calcination divided by 60 liters, the operating liquid level.

Table 2.3 Phosphate Glasses Incorporating TBP-25 Waste Oxides

TBP-25 Waste (M): 6.60 NO₃⁻, 1.72 Al³⁺, 1.26 H⁺, 0.10 Na⁺,
0.05 NH₄⁺, 0.003 Fe³⁺, 0.002 Hg²⁺, 0.003 Ru

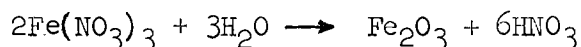
Melt	1	2	3	4	5	6	7
Additives (moles/liter)							
NaH ₂ PO ₂ ·H ₂ O	2.0	2.0	2.0	2.0	2.0	2.0	2.0
Na ₂ B ₄ O ₇ ·10 H ₂ O	0.065	0.065	---	0.032	---	---	---
NaOH	0.060	---	1.20	0.025	---	---	---
MgO	---	0.30	---	---	---	---	---
SiO ₂	---	---	0.52	0.26	---	---	---
PbO	---	---	---	---	0.125	0.188	0.250
Melt composition (wt % theoretical oxides)							
Al ₂ O ₃	28.4	28.4	26.7	27.6	27.1	26.0	25.0
Na ₂ O	22.7	22.4	20.4	21.4	20.2	19.4	18.6
P ₂ O ₅	45.9	46.0	43.3	44.6	43.9	42.1	40.5
B ₂ O ₃	2.9	2.9	---	1.4	---	---	---
SiO ₂	---	---	9.5	4.9	---	---	---
PbO	---	---	---	---	8.6	12.4	15.9
MgO	---	0.2	---	---	---	---	---
Fe ₂ O ₃	0.07	0.07	0.07	0.07	0.07	0.07	0.06
RuO ₂	0.01	0.01	0.01	0.01	0.01	0.01	0.01
Softening point (°C)	875	900	1000	950	975	925	900
Bulk density (g/ml)	2.36	2.45	2.36	2.38	2.71	2.75	2.84
Waste oxides in glass (wt %)	29.5	29.5	27.8	28.7	28.2	27.1	26.0
Volume reduction (vol TBP-25/vol glass)	7.6	7.9	7.2	7.5	8.4	8.2	8.1
Appearance	Pale yellow- ish clear glass	Pale green- ish white glass	Grayish green glass	Grayish green glass	Green glass, mottled with white	Green glass	Green- ish white glass

Fluxing agents used to form melts were borate and lead oxide. Borate was added as tetraborate, B_4O_7 , and lead oxide as PbO . Lead oxide did not lower the viscosity and softening point of melts as well as borate. However, a big advantage of lead oxide is that it does not cause foaming of the mixture prior to melting as does borate. Another advantage of lead oxide is that it yields higher density melts for the weight of additives required than do other chemicals studied. This also implies greater volume reductions. Other additives briefly investigated were magnesia and silica. Silica has the distinct disadvantage that it forms a precipitate in the original solution. Phosphate was added as NaH_2PO_2 , 2 moles per liter of waste. Other studies showed that this amount of hypophosphite is needed to hold the Ru in the condensate to $< 1\%$ of the total amount in the waste.

Ruthenium Volatility. The use of hypophosphite for controlling ruthenium volatility is particularly attractive since it is oxidized to phosphate, a glass-forming agent. The addition of at least 2 moles of sodium hypophosphite per liter of TBP-25 waste held ruthenium in the condensate during evaporation-condensation to $< 1\%$ of that in the feed. The addition of lead as a fluxing agent as $Pb(NO_3)_2$ increased the nitrate in the waste and increased ruthenium in the condensate, while addition of PbO decreased the acidity and did not materially affect the ruthenium in the condensate. The calcinations were carried to about $1000^\circ C$ in small all-quartz equipment described previously (1) with a 200-ml stainless steel beaker for a pot. Simulated TBP-25 waste (Table 2.1) containing 0.027 mg/ml stable ruthenium and 0.1 μc of Ru-106 tracer per milliliter was used.

In two experiments 2.0 moles of $NaH_2PO_2 \cdot H_2O$ was added per liter of waste. Ruthenium in the condensate was 0.48 and 0.71%, respectively, of the original ruthenium. In a third experiment 2.0 moles of $NaH_2PO_2 \cdot H_2O$ plus 0.25 mole of $Pb(NO_3)_2$ were added per liter of waste. Ruthenium in the condensate was 2.18% of the original. In a fourth experiment 2.0 moles $NaH_2PO_2 \cdot H_2O$ plus 0.25 mole PbO were added per liter of waste. Ruthenium in the condensate was 0.68% of the original. In none of the experiments was any detectable net off-gas produced.

Nitrate-Phosphite Reaction Products. The nature of the noncondensable gaseous products of the reaction between nitrate salts and orthophosphorous acid was not significantly different from those of the previously reported (2) HNO_3 - H_3PO_3 reactions. The principal product was NO , while the second most abundant was NO_2 (Table 2.4). Small amounts of N_2 and N_2O were present. The evolution of noncondensable gases started at $120 - 130^\circ C$, compared to $\sim 110^\circ C$ in the nitric-phosphorous acid reaction. The distillate was more than 6 N HNO_3 at this point. Reaction was not complete when the experiment was terminated because of phosphorous acid decomposition. At $200^\circ C$ the mixtures were still evolving gas and still contained appreciable amounts of the reducing agent. It is postulated that, at the reacting temperature, the salt nitrates hydrolyze to produce nitric acid, e.g.



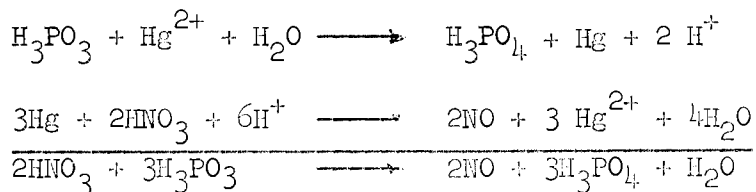
which then reacts with the phosphorous acid.

Table 2.4. Reaction of Nitrate with Phosphite

Reaction Mixture (moles/liter)					Noncondensable Off-Gas (moles/liter of mix)				Calc. H_3PO_3 for NO_3^- Reduction (moles)
HNO_3	H_3PO_3	$\text{Al}(\text{NO}_3)_3$	$\text{Fe}(\text{NO}_3)_3$	$\text{Hg}(\text{NO}_3)_2$	N_2	N_2O	NO	NO_2	
--	1.0	2.0	--	--	0.019	0.008	0.332	0.216	0.74
--	1.0	--	2.0	--	0.032	0.001	0.432	0.212	0.92
3.0	1.0	--	1.0	--	0.025	0.003	0.491	0.261	1.01
--	1.0	--	1.0	0.01	0.030	0.001	0.582	0.036	1.06

The experiments were carried out in all-glass equipment (2) with flexible polyethylene bags, connected to the system at a point between the two condensers, to collect the noncondensable off-gases. In each experiment 1 liter of reaction mixture was placed in the flask, the system was thoroughly flushed with argon, and the mixture was heated to about 200°C, the decomposition temperature of orthophosphorous acid. The off-gas passed through a nearly horizontal condenser to a downdraft condenser, and the condensate was collected in a 200-ml flask maintained at 80-90°C. The bags were calibrated to give volume as a function of gas pressure. Samples of the noncondensable gases were taken in evacuated gas sampling tubes for gas chromatographic analysis for A, N_2 , N_2O , and NO; the amount of NO_2 was calculated by difference. Samples of the condensate and the residue were taken periodically for nitrate and nitrite determinations, and samples of the residue were analyzed for phosphate and phosphite.

The use of 0.01 M $\text{Hg}(\text{NO}_3)_2$ as a catalyst (Table 2.5) caused the nitrate-phosphite reaction to occur at a lower temperature and higher rate, and the noncondensable gases were almost exclusively nitric oxide, a product characteristic of mercury reduction of the nitrate ion at low hydrogen ion concentrations. Silver and palladium* ions were also good catalysts. Although exact studies were not attempted, the mechanism of the catalysis appears to be reduction of the cation by the phosphite ion followed by oxidation of the reduced form by the nitric acid present. Many of the cations which did not catalyze the reaction are either not reduced by phosphorous acid or are not oxidized by nitric acid. A hypothetical sample of such a redox catalyst mechanism is



In the exploratory experiments to investigate the catalysis, 0.0005-0.01 mole of the material under investigation was added to 100 ml of the reaction

*All radioactive wastes will contain palladium both as a fission product and from the decay of Ru-106.

Table 2.5. Catalysis of Nitrate-Phosphite Reaction

Expt. No.	Reaction Mixture (moles/liter)			Additive (moles/liter)	Apparent Catalysis	Additional Observations
	HNO ₃	Fe(NO ₃) ₃	H ₃ PO ₃			
1	3.0	---	1.0	0.01 HgCl	No	Incomplete solution
2	3.0	---	1.0	0.01 PbO	No	Incomplete solution
3	3.0	---	1.0	0.01 CuCl	No	Bright blue solution
4	3.0	---	1.0	0.01 Hg(NO ₃) ₂	Yes	Gray ppt formed early, later dissolved
5	3.0	---	1.0	0.001 Hg(NO ₃) ₂	Yes	Same as (4) except later ppt
6	3.0	---	1.0	0.01 AgNO ₃	Yes	Dissolved to form gray colloidal ppt which dissolved upon heating
7	3.0	---	1.0	0.01 RuCl _x	No	Deeply colored solution
8	3.0	---	1.0	0.01 Ru	No	Ru metal did not appear to dissolve
9	---	1.0	1.0	0.01 Hg(NO ₃) ₂	Yes	Very vigorous gas evolution
10	---	1.0	1.0	0.01 AgNO ₃	Yes	Vigorous gas evolution
11	---	1.0	1.0	0.01 Ce(NO ₃) ₃	No	
12	---	1.0	1.0	0.01 Mn(NO ₃) ₂	No	
13	---	1.0	1.0	0.01 FeSO ₄	?	Reaction not so vigorous as with Hg ⁺⁺ but appeared to be some catalysis
14	---	1.0	1.0	0.01 I	?	Purple fumes made observation difficult
15	---	1.0	1.0	0.01 BiONO ₃	No	
16	---	1.0	1.0	0.01 AuCl ₃	No	Colloidal ppt formed, on gentle heating did not dissolve
17	3.0	---	1.0	0.005 RhCl ₃	No	
18	3.0	---	1.0	0.004 Pd(NO ₃) ₂	Yes	Metal plated out, then ppt as black spongy mass, which dissolved with vigorous gas evolution
19	3.0	---	1.0	0.005 Pd(NO ₃) ₂	Yes	Gray ppt formed, dissolved on heating; gases nearly colorless

mixture in a 150-ml Pyrex beaker. The mixture was stirred and allowed to stand ~ 15 min at room temperature and heated to boiling. Purely qualitative observations were then made as to the presence or absence of catalysis. An attempt was also made to estimate the nature of the gases being produced.

2.3 Properties of Waste Solutions (W. E. Clark, H. W. Godbee)

Vapor-liquid equilibrium, density, and boiling point data are needed in the design of the hot pilot plant to define evaporator operating conditions and to size the evaporation and rectification equipment. Vapor-liquid equilibrium for representative TBP-25, Darex, and high-sulfate Purex simulated waste solutions (Table 2.6), determined in Gillespie still distillations, and pot liquid densities are shown in Tables 2.7-2.9. The intended goal was to investigate solutions ranging in metal concentration from one-half to twice that of the so-called "standard" compositions (Table 2.1). This goal was not always attainable due to instability of the more concentrated solutions. Four different acid concentrations were investigated at each salt concentration, although here, also, solution instability sometimes prevented study of the more concentrated solutions. Each solution was equilibrated twice, once at atmospheric pressure (744-751 mm Hg) and again at 559-569 cm Hg.

2.4 Design of Hot Cell Evaporation-Calcination Equipment (J. O. Blomeke and H. O. Weeren)

Installation of equipment for evaporating and calcining actual waste solutions in a hot cell, in order to obtain information on the volatility of fission products, the buildup of pressure in the calciner pot after calcination due to radiation decomposition, and the distribution of fission products in the solids. The proposed calciner pot dimensions are 4 in. dia by 24 in. high, and the maximum size of the feed batch, as determined by the capacity of the available waste carrier, will be 5 gal. The calciner pot dimensions are the same as the dimensions of the calciner pot used in nonradioactive laboratory tests, since the results obtained there were found to be partly dependent on pot size and geometry. If a smaller-scale test appears desirable, a 2.5-in.-dia pot can be substituted without alteration to the rest of the equipment.

A series of several runs in the hot cell is currently contemplated. Besides the necessary break-in runs with nonradioactive and low-activity-level feeds, there will be several runs on feed material from Idaho and two or more runs on Hanford waste. Runs with locally produced wastes can be performed in addition to or in place of those with imported wastes, depending on the availability and suitability of the local wastes for this work.

The waste solution will be brought from Idaho or Hanford in a recently designed 5-gal liquid waste carrier. The carrier will be placed in an enclosed box on the roof of the cell and the waste solution transferred to the transfer tank by vacuum (Fig. 2.3). When transfer is complete, the waste solution will be dropped to the feed tank and the carrier will be washed and removed. The solution in the feed tank will be agitated by continuously pumping a 0.5-gpm stream out of and back into the tank. A stream of up to 100 ml/min will be pumped to the calciner pot. A separate line from outside the cell will be used to feed calcium solutions to the calciner pot when desired. A water flush will be used on both feed lines after each transfer

Table 2.6 Compositions of Simulated Waste Solutions

Solution No.	Solution Composition (M)										
	H ⁺	Al ³⁺	Fe ³⁺	Na ⁺	Hg ⁺⁺	NO ₃ ⁻	Cr ³⁺	Ni ⁺⁺	SO ₄ ⁼	Mn ⁺⁺	Cl ⁻
A. TBP-25 Waste											
T-1	1.26	1.72	0.003	0.01	0.02	6.48					
-1a	0.5	1.72	0.003	0.01	0.02	5.72					
-1b	3.0	1.72	0.003	0.01	0.02	8.22					
-1c	5.0	1.72	0.003	0.01	0.02	10.22					
T-2	1.26	0.86	0.0015	0.005	0.01	3.87					
T-2a	0.5	0.86	0.0015	0.005	0.01	3.11					
2b	3.0	0.86	0.0015	0.005	0.01	5.61					
2c	5.0	0.86	0.0015	0.005	0.01	7.61					
T-3*	1.26	3.44	0.006	0.02	0.04	11.7					
3a*	0.5	3.44	0.006	0.02	0.04	10.94					
3b*	3.0	3.44	0.006	0.02	0.04	13.44					
3c*	5.0	3.44	0.006	0.02	0.04	15.44					
T-4**	1.26	2.6	0.0045	0.015	0.03	9.15					
4a*	0.5	2.6	0.0045	0.015	0.03	8.39					
4b*	3.0	2.6	0.0045	0.015	0.03	10.89					
4c*	5.0	2.6	0.0045	0.015	0.03	12.89					
B. High-sulfate Purex Waste											
PS-1	5.6	0.1	0.5	0.6		6.05	0.01	0.01	1.0		
1a	7.0	0.1	0.5	0.6		7.45	0.01	0.01	1.0		
1b	4.0	0.1	0.5	0.6		4.45	0.01	0.01	1.0		
1c	2.0	0.1	0.5	0.6		2.45	0.01	0.01	1.0		
PS-2	5.6	0.05	0.25	0.3		5.825	0.005	0.005	0.5		
2a	7.0	0.05	0.25	0.3		7.225	0.005	0.005	0.5		
2b	4.0	0.05	0.25	0.3		4.225	0.005	0.005	0.5		
2c	2.0	0.05	0.25	0.3		2.225	0.005	0.005	0.5		
PS-3	5.6	0.2	1.0	1.2		6.50	0.02	0.02	2.0		
3a	7.0	0.2	1.0	1.2		7.90	0.02	0.02	2.0		
3b	4.0	0.2	1.0	1.2		4.90	0.02	0.02	2.0		
3c	2.0	0.2	1.0	1.2		2.90	0.02	0.02	2.0		
C. Darex Waste											
D-1	2.001		1.21			7.19	0.38	0.17		0.04	0.001
1a	3.002		1.21			8.19	0.38	0.17		0.04	0.001
1b	5.003		1.21			10.19	0.38	0.17		0.04	0.001
1c	7.004		1.21			12.19	0.38	0.17		0.04	0.001
D-2	2.001		0.6			4.58	0.19	0.085		0.02	0.0005
2a	3.002		0.6			5.58	0.19	0.085		0.02	0.0005
2b	5.003		0.6			7.58	0.19	0.085		0.02	0.0005
2c	7.004		0.6			9.58	0.19	0.085		0.02	0.0005
D-3*	2.001		2.42			12.38	0.76	0.34		0.08	0.002
3a*	3.002		2.42			13.38	0.76	0.34		0.08	0.002
3b*	5.003		2.42			15.38	0.76	0.34		0.08	0.002
3c*	7.004		2.42			17.38	0.76	0.34		0.08	0.002
D-4	2.001		1.82			9.80	0.57	0.255		0.06	0.0015
4a	3.002		1.82			10.80	0.57	0.255		0.06	0.0015
4b	5.003		1.82			12.80	0.57	0.255		0.06	0.0015
4c*	7.004		1.82			14.80	0.57	0.255		0.06	0.0015

* These solutions could not be made up due to solubility limitations.

** This solution was not stable at room temperature.

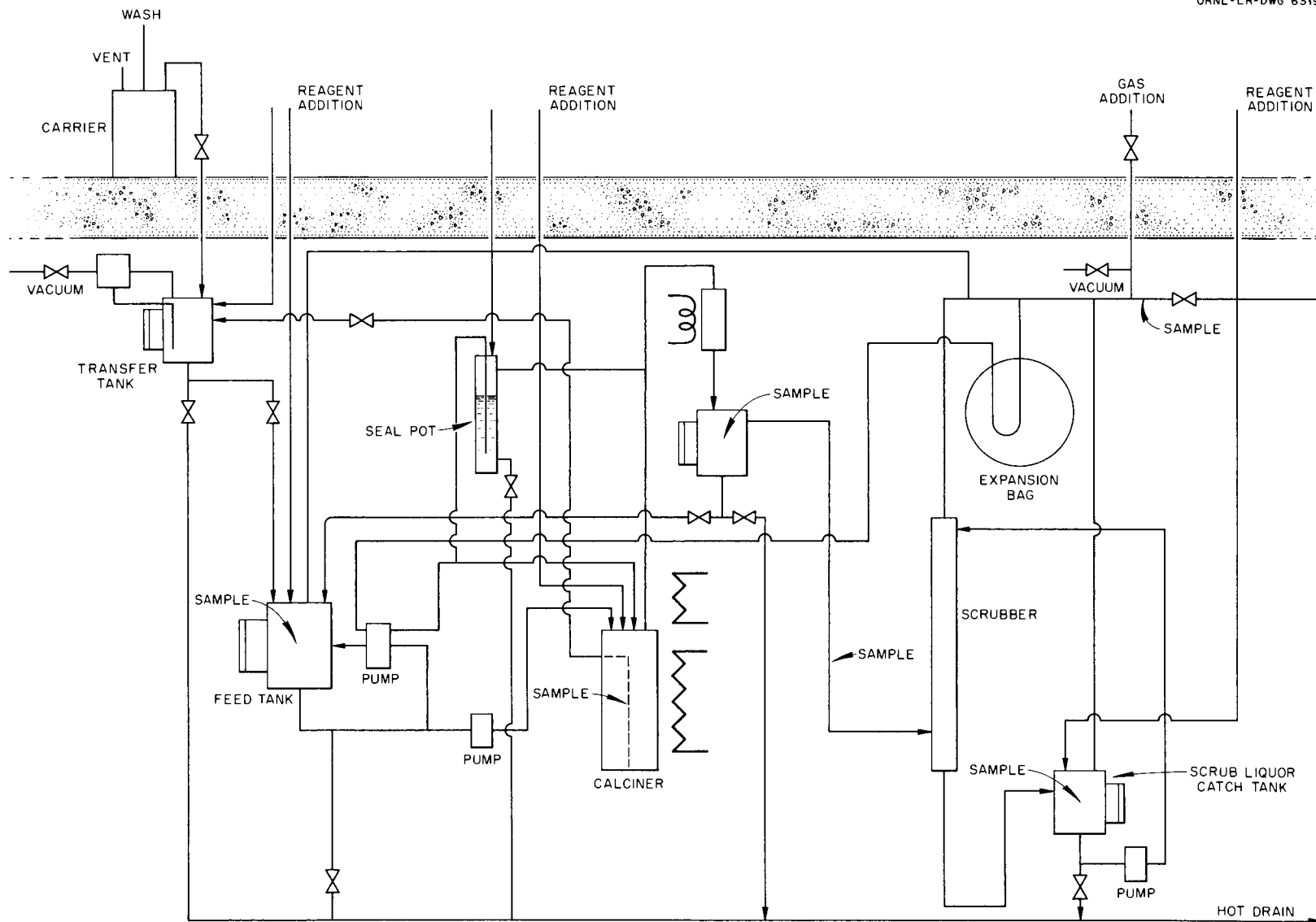


Table 2.7. Vapor-Liquid Equilibrium and Density Data for Simulated TBP-25 Waste

Solution	H ⁺ , Analyzed (M)	Equilibrium Boiling Point (°C)	Absolute Pressure (mm Hg)	Density (g/ml)			
				25°C	50°C	75°C	100°C
T-1	1.26	109.5	748.3				
pot	1.28			1.3238	1.3072	1.2818	1.2688
distillate	0.52						
T-1 (Duplicate)	1.32	109.5	747.1				
pot	1.35			1.3194	1.3049	1.2885	1.2672
distillate	0.52						
T-1a	0.50	107.5	748.3				
pot	0.58			1.2963	1.2819	1.2580	1.2443
distillate	0.15						
T-1b	2.91	113.5	748.5				
pot	2.96			1.3725	1.3512	1.3317	1.3124
distillate	2.10						
T-1c	4.85**	117	746.3				
pot	4.86			1.4249	1.4034	1.3811	1.3574
distillate	5.45						
T-2	1.26	104	746.3				
pot	1.34			1.1922	1.1803	1.1593	1.1341
distillate	0.13						
T-2a	0.50	102.5	746.4				
pot	0.54			1.1669	1.1531	1.1361	1.1087
distillate	0.04						
T-2b	2.97	107.5	746.6				
pot	3.17			1.2478	1.2319	1.2131	1.1833
distillate	0.60						
T-2c	4.96	111.5	745.7				
pot	5.10			1.3039	1.2811	1.2609	1.2385
distillate	2.01						
T-4*		117	746.6				
pot	1.26						
distillate	1.92						
T-4-1*		119	745.7				
pot	2.22						
distillate	4.11						
T-4-2*		120.5	745.7				
pot	3.03						
distillate	6.24						
T-4-3*		121.5	744.8				
pot	3.70						
distillate	8.24						
T-4-4*		122	744.8				
pot	4.22						
distillate	9.84						
T-4-5*		122.5	744.8				
pot	4.64						
distillate	11.00						

Table 2.7 (Cont.)

Solution	H ⁺ , Analyzed (M)	Equilibrium Boiling Point (°C)	Absolute Pressure (mm Hg)	Density (g/ml)			
				25°C	50°C	75°C	100°C
T-1s	1.26	101.5	567.5				
pot	1.32			1.3242	1.3099	1.2938	1.2710
distillate	0.51						
T-1s (Duplicate)	1.32	102	563.9				
pot	1.41			1.3279	1.3141	1.2963	1.2731
distillate	0.58						
T-1as	0.50	100	566.7				
pot	0.56			1.2961	1.2837	1.2632	1.2443
distillate	0.17						
T-1bs	2.91	105	566.7				
pot	3.02			1.3699	1.3522	1.3339	1.3102
distillate	2.03						
T-1cs**	4.85	110	---				
pot	5.12			1.4286	1.4069	1.3842	1.3589
distillate	5.95						
T-2s	1.26	96	567.5				
pot	1.41			1.1914	1.1786	1.1581	1.1320
distillate	0.58						
T-2as	0.50	94	566.7				
pot	1.34			1.1647	1.1532	1.1344	1.1087
distillate	0.092						
T-2bs	2.97	99	566.7				
pot	3.21			1.2444	1.2295	1.2110	1.1800
distillate	0.51						
T-2cs	4.96	104	---				
pot	5.25			1.3041	1.2818	1.2603	1.2356
distillate	1.88						
T-4s*		109	566.4				
pot	1.26						
distillate	1.86						
T-4-1s		111.5	566.4				
pot	2.22						
distillate	3.83						
T-4-2s		113	563.9				
pot	3.03						
distillate	5.89						
T-4-3s		113.5	563.9				
pot	3.70						
distillate	7.81						

* T-4 was not stable at room temperature. In order to obtain equilibrium data on this and the following solutions, concentrated acid was added to the pot after each distillation. Pot compositions for T-4b through T-4f are therefore calculated values.

** Apparent analytical error probably due to solution instability at room temperature.

Table 2.8. Vapor-Liquid Equilibrium and Density Data for Simulated Purex Waste

Solution	H ⁺ , Analyzed (M)	Equilibrium Boiling Point (°C)	Absolute Pressure (mm Hg)	Density (g/ml)			
				25°C	50°C	75°C	100°C
PS-1	5.35	110.5	---				
pot	5.52			1.3175	1.2994	1.2773	1.2505
distillate	1.43						
PS-1a	6.75	113	747.7				
pot	6.88			1.3194**	1.2991	1.2769	1.2497
distillate	2.81			1.3175	1.2994	1.2773	1.2505
PS-1b	3.70	107.5	747.7				
pot	3.92			1.2736	1.2565	1.2377	1.2106
distillate	0.58						
PS-1c	1.88	104	750.5				
pot	1.91			1.2115	1.1974	1.1804	1.1536
distillate	0.091						
PS-2	5.50	109	747.7				
pot	5.57			1.2653	1.2470	1.2246	1.1947
distillate	1.10						
PS-2a	6.78	111	747.7				
pot	6.89			1.2944	1.2738	1.2376	1.2217
distillate	2.12						
PS-2b	3.80	106	750.5				
pot	4.08			1.2133	1.1973	1.1776	1.1487
distillate	0.44						
PS-2c	1.82	103	750.5				
pot	1.95			1.1423	1.1297	1.1129	1.0800
distillate	0.058						
PS-3*	5.25	113	750.4				
pot	5.36			1.4470	1.4272	1.4032	1.3770
distillate	2.67						
PS-3a	6.67	116	750.4				
pot***	6.81						
distillate	4.88						
PS-3b	3.67	110	744.4				
pot	3.77			1.3991	1.3810	1.3603	1.3334
distillate	1.05						
PS-3c	2.22	106.5	747.5				
pot	2.38			1.3778	1.3612	1.3426	1.3144
distillate	0.25						

Table 2.8 (Cont.)

Solution	H ⁺ , Analyzed (M)	Equilibrium Boiling Point (°C)	Absolute Pressure (mm Hg)	Density (g/ml)			
				25°C	50°C	75°C	100°C
PS-1s	5.35						
pot	5.53	101	563.6				
distillate	0.95			1.3319	1.3103	1.2845	1.2508
PS-1as	6.75	105	567.1				
pot	6.73			1.3543	1.3324	1.3076	1.2777
distillate	2.42						
PS-1bs	3.70	99.5	567.1				
pot	3.83			1.2747	1.2575	1.2376	1.2114
distillate	0.44						
PS-1cs	1.88	96	566.6				
pot	1.85			1.2104	1.1963	1.1791	1.1480
distillate	0.056						
PS-2s	5.50	103.5	563.6				
pot	5.38			1.2663	1.2474	1.2252	1.1950
distillate	1.49						
PS-2as	6.78	103	567.1				
pot	6.66			1.2953	1.2725	1.2469	1.2167
distillate	1.94						
PS-2bs	3.80	98.5	567.1				
pot	3.92			1.2131	1.1959	1.1773	1.1451
distillate	0.37						
PS-2cs	1.82	95	566.6				
pot	1.87			1.1457	1.1331	1.1150	1.0884
distillate	0.048						
PS-3s	5.25	106	566.6				
pot	5.63			1.4552	1.4331	1.4112	1.3833
distillate	2.64						
PS-3bs	3.67	103	566.6				
pot	4.17			1.4037	1.3844	1.3639	1.3395
distillate	0.99						
PS-3cs	2.22	99	566.6				
pot	2.16			1.3777	1.3602	1.3416	1.3155
distillate	0.19						

* Solution precipitated on standing.

** Measurements made on duplicate samples.

*** Densities of solution not determined because of solution instability.

Table 2.9. Vapor-Liquid Equilibrium and Solution Density Data for Simulated Darex Waste

Solution	H ⁺ , Analyzed (M)	Equilibrium Boiling Point (°C)	Absolute Pressure (mm Hg)	Density (g/ml)			
				25°C	50°C	75°C	100°C
D-1	1.83	110	746.7				
pot	1.97			1.3844	1.3665	1.3470	1.3203
distillate	0.94						
D-1a	2.75	112.5	747.1				
pot	2.99			1.4129	1.3941	1.3727	1.3469
distillate	1.86						
D-1b	4.41*	116	750.4				
pot	4.92			1.4595	1.4370	1.4126	1.3829
distillate	4.46						
D-1c	6.70	119	750.4				
pot	6.80			1.5080	1.4813	1.4485	1.4175
distillate	8.51						
D-2	1.88	105.5	747.1				
pot	2.06			1.2380	1.2200	1.2011	1.1732
distillate	0.26						
D-2a	2.80	107.5	750.4				
pot	3.11			1.2731	1.2555	1.2374	1.2149
distillate	0.59						
D-2b	4.77	111	750.4				
pot	5.16			1.3289	1.3077	1.2746	1.2602
distillate	1.81						
D-2c	6.39	114.5	749.3				
pot	7.05			1.3765	1.3513	1.3237	1.2947**
distillate	4.02			1.3764	1.3514	1.3260	1.2965
D-4***		117	749.3				
pot	1.98			1.5363	1.5167	1.4869	1.4650
distillate	3.19						
D-4a***		118.5	750.1				
pot	2.75			1.5563	1.5356	1.5100	1.4814
distillate	4.74						
D-4b***		121	750.1				
pot	4.58			1.5841	1.5598	1.5319	1.4992
distillate	8.57						

Table 2.9 (Cont.)

Solution	H ⁺ , Analyzed (M)	Equilibrium Boiling Point (°C)	Absolute Pressure (mm Hg)	Density (g/ml)			
				25°C	50°C	75°C	100°C
D-1s	1.83						
pot	1.97						
distillate	0.80			1.3874	1.3701	1.3455	1.3265
D-1as	2.75	105	566.0				
pot	2.90			1.4168	1.3993	1.3763	1.3506
distillate	1.66						
D-1bs	4.41	108.5	562.4				
pot	4.86			1.4628	1.4396	1.4040	1.3847
distillate	4.12						
D-1cs	6.70*	111.5	559.8				
pot	6.87			1.5101	1.4831	1.4537	1.4216
distillate	8.10						
D-2s	1.88	97.5	566.0				
pot	2.00			1.2300	1.2151	1.1908	1.1707
distillate	0.20						
D-2as	2.80	99.5	566.0				
pot	3.09			1.2709	1.2539	1.2354	1.2063
distillate	0.53						
D-2bs	4.77	103	562.4				
pot	5.18			1.3257	1.3066	1.2838	1.2573
distillate	1.67						
D-2cs	6.39	106.5	559.8				
pot	7.07			1.3768	1.3529	1.3269	1.2961
distillate	3.79						
D-4***		109.5	568.1				
pot	1.94			1.5320	1.5117	1.4873	1.4587
distillate	2.91						
D-4as***		111	568.1				
pot	2.84			1.5582	1.5352	1.5104	1.4802
distillate	4.72						
D-4bs***		113.5	568.1				
pot	4.50			1.5842	1.5580	1.5293	1.4970
distillate	8.18						

* Apparent analytical error.

** Duplicate determinations.

*** Not stable at room temperature.

to prevent plugging. A third line feeding the calciner pot is a gas circulation line that serves the additional function of an emergency vent.

During the first stage of a run the waste solution will be concentrated in the calciner pot by boiling. The vapor will be discharged through a vent line to a condenser, and the noncondensables will be sent through a scrubber and then recycled to the calciner pot. The liquid level in the calciner pot will be maintained by regulating the feed rate and will be determined by thermocouple readings.

After evaporation is complete, the calciner pot will be heated to 900°C , during which mercury is expected to be driven off from TBP-25 wastes, to the piping between the top of the pot, and the disconnects will be kept at a temperature above the condensation temperature (450°C) of the mercury compounds. Off-gas flow will be the same as in the first stage of the run, i.e., through a condenser, a scrubber, and back to the calciner pot.

When calcination is complete and the pot has cooled, the furnaces will be swung aside and the calciner disconnected from the equipment. The feed and vent lines on the pot will be sealed and the pot withdrawn from the cell through a hole in the roof, into a transfer carrier, and elsewhere for observation and ultimate disposal. A new calciner pot will then be lowered into place and connected to the equipment for the next run.

For the study of ruthenium behavior during evaporation a calciner pot of slightly different design will be substituted. It will be connected to the equipment and partially filled with waste solution, and the condensate collected during the previous calcination run will then be dropped to the feed tank. The waste solution in the calciner will be brought to a boil and the condensate in the feed tank pumped in at the evaporation rate until all the condensate has been used. The ruthenium distribution between evaporator solution and condensate can then be determined by analyses.

Because one of the main purposes of the hot cell tests is to determine the volatility of fission products from actual waste solutions, it is necessary that believable mass balances be obtained. Since analysis of the calcined cake is extremely difficult even when there is no activity present and would be almost impossible for high-activity wastes, a mass balance for all volatile fission products will have to be obtained by analyzing the feed solution at the start of a run and the condensate and scrub liquor at the end of a run. Since ruthenium, in particular, tends to plate out on any surface at hand, the vent line between the calciner pot and the condenser will be decontaminated after each run and the decontaminating solution analyzed for volatile fission products.

Any pressure buildup in the calciner pots after they are removed from the cell will be noted on a pressure gage connected to one of the vent lines, and comparison of this reading with pot temperature will indicate how much of the pressure rise is due to gas generation inside the pot.

Provision will be made to run the experiment with a nitric oxide gas blanket to determine the effect of this variable, if desired.

2.5 Design of Calcination Pilot Plant (J. O. Blomeke, J. M. Holmes, E. J. Frederick)

Preparation of flowsheets for the ICPP waste calcination pilot plant is under way. A total of eight will be made, one batch and one continuous for each of the TBP-25, Darex, high-sulfate Purex, and low-sulfate Purex processes. The TBP-25 waste flowsheet is receiving prime attention since its calcination will be tested first at Idaho. However, since the equipment must be sized for maximum flow rates, feed rates for all the processes must be determined before equipment design can be started. The furnace will be designed to handle 6-, 8-, or 12-in.-dia pots with an active length of 6 ft. Over-all pot length will be 7.5 - 8 ft. The process equipment sizes will be determined by the 12-in.-dia pot size.

The off-gas equipment shown on the flowsheet in the initial proposal (3) will be simplified by omitting the gas holder and blower used to recycle gas to the acid scrubber for removal of absorbable oxides of nitrogen. Nitric oxide generated during the addition of phosphite to the process or used to purge the evaporator to minimize ruthenium volatility may necessitate the use of the acid scrubber to absorb excess off-gas after conversion of the nitric oxide to absorbable nitrogen dioxide. This provision will minimize the net volume of off-gas generated by the calcination pilot plant.

Design of mechanical equipment for demonstration of the pot calciner positioning, connecting, and sealing procedures is about 60% complete. The equipment is sized for either the Lockheed Nuclear Products cells at Dawsonville, Georgia or the ICPP Hot Pilot Plant Cell 2. A contract for the demonstration has been signed with the Lockheed Company, and work started on Oct. 1. Bid invitations for construction of the demonstration equipment are being issued, and equipment fabrication should start in November.

3.0 LOW-LEVEL WASTE TREATMENT

A scavenging-ion exchange process (4, 5) is being developed for decontaminating the large volumes of slightly contaminated water produced in nuclear installations; ORNL low-activity-level waste is being used as a medium for study. The scavenging-ion exchange process uses phenolic resins, as opposed to polystyrene resins, since the phenolic resins are much more selective for cesium in the presence of sodium; the Cs/Na separation factor is 160 for phenolic groups, and 1.5 for sulfonic groups. Other cations, e.g., strontium and rare earths, are also sorbed efficiently. Inorganic ion exchange media such as vermiculite and clinoptilolite are being studied as alternatives. The waste solution must be clarified prior to ion exchange since ion exchange media do not remove colloidal materials efficiently. Water clarification techniques are being developed for both the ion exchange processes and for the ORNL lime-soda process waste water treatment plant. Work is proceeding on both development and pilot plant programs.

3.1 Scavenging-Ion Exchange Process

Demonstration Run (W. E. Clark, R. R. Holcomb). In the last run in the semi-pilot plant facility the activity in 1500 bed volumes of waste was reduced to less than 10% of the MPC. Neither Sr nor total hardness breakthrough to the 1% level was detected up to 2000 bed volumes. In this run (SPP-8), total hardness in the overflow from the sludge-blanket clarifier averaged about 20 ppm (as CaCO_3), compared to 60 ppm in the previous run (SPP-7) in which a premature breakthrough of activity and total hardness occurred at ~600 bed volumes (see Fig. 3.1a and b and Table 3.1). Comparison of all results supports the hypothesis that the early breakthrough was caused by a carbonate deficiency in the raw water, resulting in a higher residual hardness than normal, and the soluble calcium saturated the resin. An instrument for continuous determination of total hardness in pilot plant test effluents has been installed to detect future breakthroughs of this type. It is believed that this type of breakthrough can be prevented by addition of carbonate to the water if filtered feed hardness rises above normal.

Pilot Plant (J. O. Blomeke, J. M. Holmes, W. R. Whitson, R. E. Brooksbank, W. T. McDuffee). Installation was completed of the pilot plant for demonstration of the cleanup of ORNL process waste by scavenging and ion exchange. Details of the process flowsheet were given in reference 1, pp. 37-41. Because of the simplicity of the process and equipment the continuous operation of the pilot plant will be conducted by personnel currently engaged in a plutonium-aluminum alloy program, and the shakedown tests are under way for (1) orientation of personnel and procedures; (2) leak-testing of pipelines and equipment; (3) calibration of tanks and instrumentation; (4) determination of equipment pressure drop characteristics; and (5) determination of equipment modification needed for optimum performance. With ORNL tap water for feed, ~300 hr of nonradioactive processing was accomplished at feed flow rates ranging from 7.5 to 10 gpm. The Eimco-Burwell plate-and-frame clarifier sludge filter operated satisfactorily in tests but cannot be used when the plant processes contaminated water without extensive containment modifications. Present plans call for removal of this filter when the facility goes hot. An enclosed type 3FIC vacuum filter manufactured by the Oliver United Filter Company, now being installed, has a 1-ft-dia x 1-ft-long drum and will filter the sludge effluent from the clarifier continuously. The discharge of contaminated cake from the filter into plastic bags will comply with the containment requirements for the process.

An alarm system, which monitors critical variables in the waste treatment plant, was installed in Building 4507.

3.2 Inorganic Ion Exchange of Process Waste Water Plant Effluent (K. E. Cowser)

Heat Treatment of Grundite. Studies by Tamura have shown that heat treatment of Grundite to 600°C improves its ability to remove cesium from solutions of 1.5 M NaNO_3 . In slurry and settling tests, Grundite heated to 600°C for various periods of time increased Cs-137 removals from 83% to 96% in synthetic waste and from 88% to 96% in spiked tap water (Table 3.2). For a particle size of less than 8-10 μ dia, heat treatment reduced the percent of fines a factor of 1.5 to 2 (Fig. 3.2). The slurry tests consisted

Table 3.1. Decontamination of Low-Level Waste in Demonstration Runs SPP-7 and 8

Code*	Activities						
	c ml ⁻¹ min ⁻¹		d ml ⁻¹ min ⁻¹				
	Gr β	Gr γ	Gr β	TRE	Sr	Cs	Co
Run SPP-7							
F-100 bed vol			351.60	141.78	129.85	86.76	46.43
FF-100			229.1	47.41	85.23	19.26	1.84
Eff-100			16.67	0.344	0.01	n.d.	1.62
F-500 bed vol			460.30	146.85	151.42	111.20	76.19
FF-500			229.1	43.87	100.80	39.96	3.03
Eff-500			25.00	0.411	0.56	0.36	1.81
Eff-600 bed vol			----	----	8.59	1.08	1.46
Eff-700 bed vol			----	----	29.9	3.25	4.47
Eff-800 bed vol			----	----	59.59	5.30	10.12
Eff-900 bed vol			----	----	80.72	7.79	6.65
F-1000 bed vol			304.70	96.04	159.81	66.06	46.76
FF-1000			134.60	36.39	70.11	52.56	10.14
Eff-1000			123.20	44.73	95.24	7.61	8.01
Eff-1200 bed vol			----	48.8	69.1	13.57	5.82
F-1500 bed vol			186.70	61.75	136.40	50.04	35.78
FF-1500			90.25	15.82	62.09	27.0	3.53
Eff-1500			81.30	14.04	52.51	25.02	3.30
F-2000 bed vol			248.30	97.52	151.13	24.52	21.68
FF-2000			69.84	20.93	49.49	19.80	2.08
Eff-2000			62.36	12.1	36.40	11.66	1.91
Run SPP-8							
F-100 bed vol	30.2	14.7		10.34	134.32	27.18	18.86
FF-1000	5.8	6.3		2.25	48.02	25.74	2.85
Eff-1000	0.3	0.92		0.015	0.0	trace	4.35
Eff-1200 bed vol	0.38	1.60		----	----	0.8	----
Eff-1300 bed vol	0.37	2.11		----	----	1.45	----
Eff-1400 bed vol	0.13	1.56		----	----	2.75	----
F-1500 bed vol	25.3	13.8		7.89	161.39	23.58	16.91
FF-1500	6.8	6.3		1.69	48.2	21.96	3.60
Eff-1500	0.43	2.3		0.024	0.05	4.82	4.64
Eff-1700 bed vol	1.3	3.01		----	----	7.48	----
F-2000 bed vol	21.1	12.4		6.92	156.20	24.84	18.60
FF-2000	5.4	5.02		1.02	41.65	22.86	3.12
Eff-2000	1.15	3.3		0.024	0.16	14.78	2.32

* F = feed; FF= precipitated-filtered feed; Eff = effluent.

UNCLASSIFIED
ORNL-LR-DWG 63194

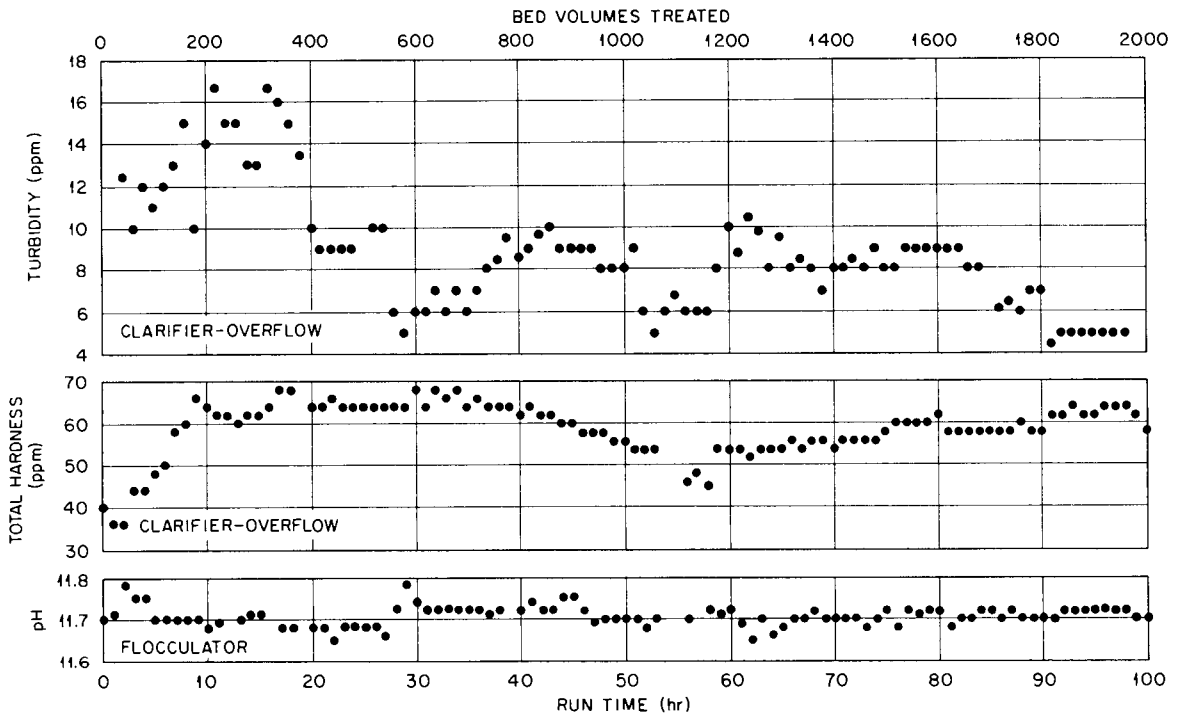


Fig. 3.1a. Data for Semi-Pilot-Plant Treatment, by Scavenging-Ion Exchange, of Process Waste Water, Run 7.

UNCLASSIFIED
ORNL-LR-DWG 63195

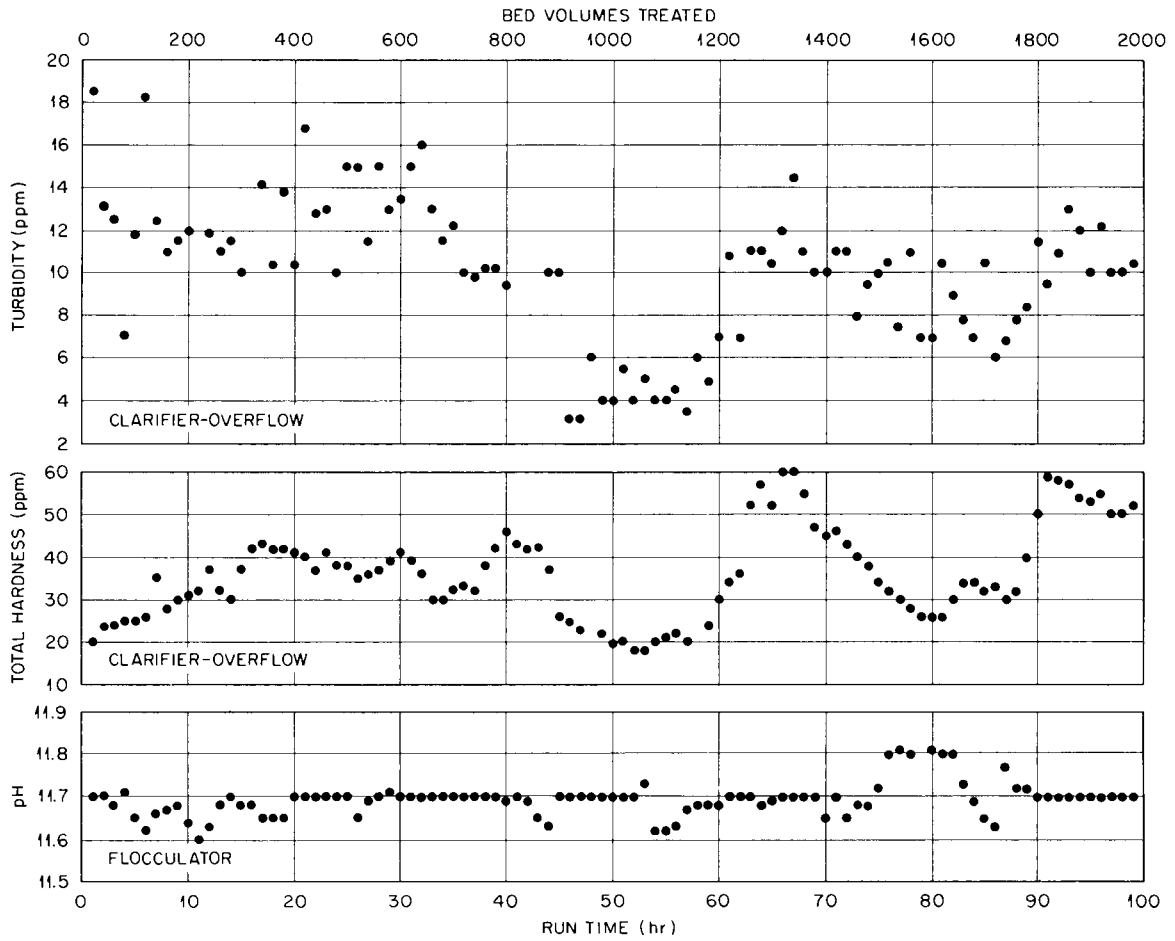


Fig. 3.1b. Data for Semi-Pilot-Plant Treatment, by Scavenging-Ion Exchange, of Process Waste Water, Run 8.

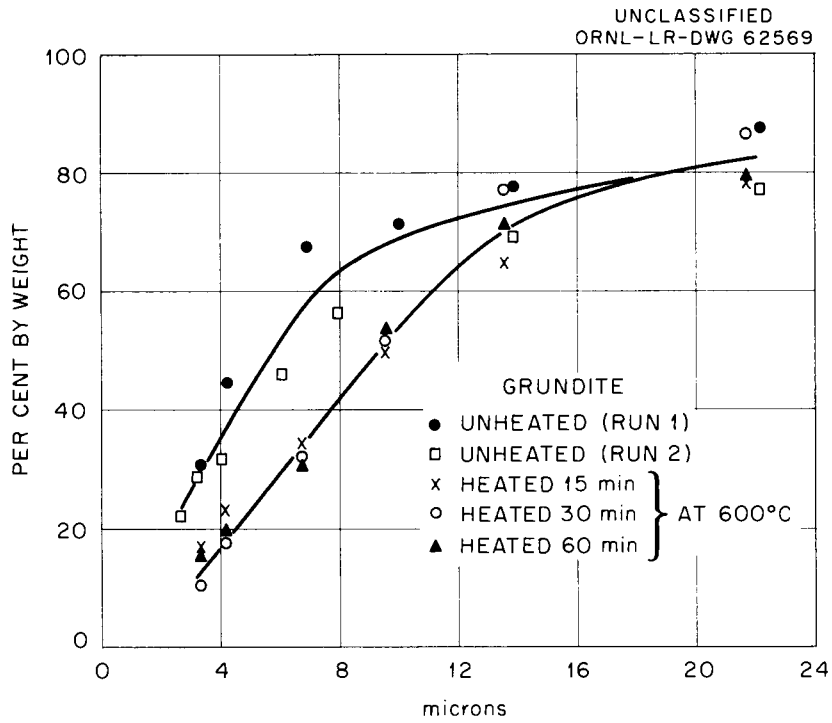


Fig. 3.2. Effect of Heat Treatment on Particle Size Distribution of Grundite.

of contacting 0.1 g of Grundite with 30 ml of tap water or 30 ml of synthetic waste for 30 and 120 min; a Cs-137 spike was used with each solution. The settling tests consisted of particle size determinations of Grundite in synthetic waste by the Andreasen pipette technique. Grundite was contacted 3¹/₄ min with the waste solution, to duplicate the time of contact in the flocculators of the treatment plant, before starting the tests.

Table 3.2. Effect of Heat Treatment on Cesium Sorption by Grundite

Heating Time (min)	Cesium Removed (%)			
	Oak Ridge Tap Water		Synthetic Waste	
	30 min contact	120 min contact	30 min contact	120 min contact
0	89.0	87.8	84.8	82.0
15	96.7	96.3	94.9	95.1
30	96.2	96.0	96.0	96.0
60	96.0	95.9	96.6	96.5

In tests by Dorr-Oliver, Inc. (runs 9-13) to classify solids in the effluent of the waste treatment plant (6), a total of 64,000 gal of waste containing 30 ppm of suspended solids was passed through the hydroclones; a smaller volume of hydroclone effluent was treated with a Merco centrifuge. The suspended solids contained 48% of the gross γ activity, 59% of the Cs-137, and 34% of the Sr-90. An average of 25% of the suspended solids was collected by the hydroclone system, the median diameter of the solids collected by the smallest unit (TM) being 7.9 μ . With the Merco centrifuge (median collection diameter 6.5 μ) handling the effluent from the hydroclones (runs 12, 13), an average of 60% of the suspended solids was collected. Of the solids collected by the hydroclones, 73 wt % was CaCO₃ (runs 11, 12), and of those collected by the centrifuge, 47 wt % was CaCO₃. Approximately 40% of the suspended solids were finer than 6.5 μ and the percentage of non-CaCO₃ solids increased as the particle size of the solids decreased.

4.0 ENGINEERING, ECONOMIC, AND HAZARDS EVALUATION

R. L. Bradshaw, J. J. Perona, J. T. Roberts

The economics of disposal of high-activity waste in salt as (1) liquids in rooms with recessed floors, (2) pot calcination vessels in racks above the floor, and (3) pot calcination vessels in holes in the floor is under study. An important variable is the amount of mine space required for safe dissipation of fission product heat. For cases 1 and 2 the infinite-slab heat calculation (2) should give an adequate estimate of space requirements (see below). For case 3 the computer code for the equation presented in reference 2 was written and is undergoing "debugging."

Results of the infinite-slab calculations for Purex waste are shown in Fig. 4.1. The uranium fuel was assumed to have been irradiated for 3×10^7 sec at a flux of 3×10^{13} at an enrichment sufficient to give 10,000 Mwd/tonne. (Thorium fuel was assumed to be irradiated for the same time at the same flux but at a U-235 content to give 20,000 Mwd/tonne.) The waste was assumed to be intimately mixed with the salt in a layer 1 ft thick, and heat dissipation was by conduction alone. Thus the peak waste temperature in the center of the slab and the peak salt temperature are the same. The three curves are the temperature rises calculated from the values of thermal conductivity and diffusivity of salt at three different temperatures.

4.1 Liquids in Salt

For liquid wastes the maximum waste temperature must be kept below boiling and thus the lower curve of Fig. 4.1 (100°C thermal properties) should be used. Assuming an ambient mine temperature of 75°F , a rise of 125°F could be allowed. Figure 4.2, derived from the lower curve of Fig. 4.1, shows the maximum allowable heat generation rate, as a function of waste age at burial, for a peak waste-and-salt temperature rise of 125°F . Figure 4.2, then, makes it possible to calculate the total mine space requirements for storing the output from processing the assumed 1500 tons/year of uranium and 270 tons/year of thorium converter fuel. The gross mine area required, as a function of decay time before disposal, is shown in Fig. 4.3. For example, wastes aged 2 to 10 years would require 21 to 16 acres/year. These curves assume that only 50% of the gross mine area is used for actual waste storage but do not take any credit for lowering the peak temperature rise because of less than 100% utilization.

4.2 Calcination Vessels above Floor

If calcination vessels are stored in racks above the floor of sealed mine rooms so that it may be assumed that all heat is transferred to the floor and ceiling by convection alone, the same infinite-slab calculation should be a reasonable approximation. Since unrestrained rock salt aggregates shatter when heated above 450 to 500°F it seems desirable to limit the salt temperature to 400°F . Assuming the 75°F ambient, this allows a rise of 325°F . From the middle curve of Fig. 4.1 and the heat generation per calcination vessel (cylinder) as a function of waste age for the various waste types, curves showing the required floor area per cylinder will be calculated.

In addition to the limit on the spacing of cylinders imposed by the salt, a limit is imposed by the requirement that the axis temperature in the cylinder should not go over 1650°F . The axis temperature was calculated by assuming that the salt temperature is 400°F and adding the temperature differentials across the can, from the can to the air, and from the air to the salt. From this calculation is found the minimum waste age for each size cylinder, below which the axis temperature limit cannot be maintained no matter how great the floor area per cylinder:

UNCLASSIFIED
ORNL-LR-DWG 62815

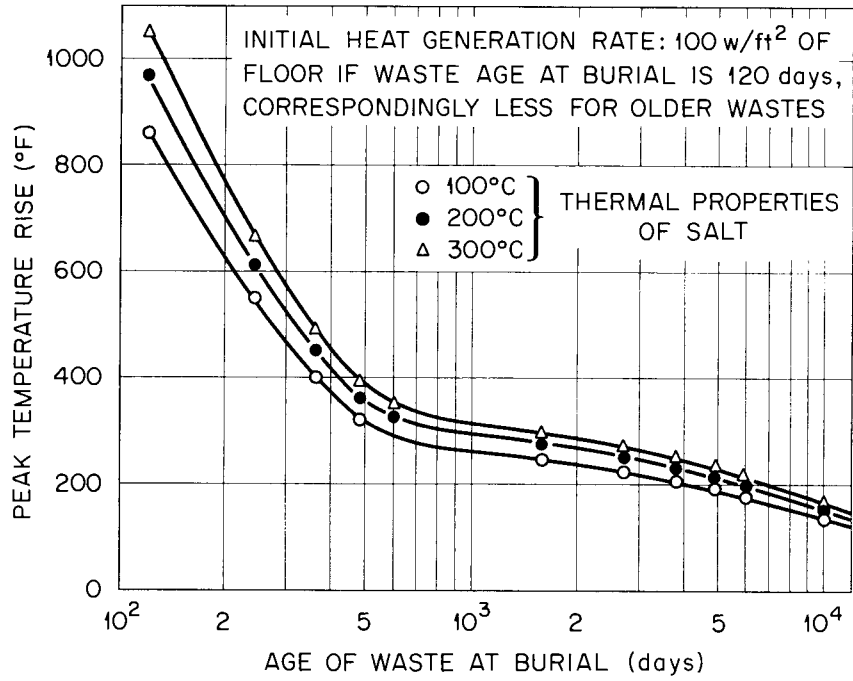


Fig. 4.1. Peak Salt Temperature Rise as a Function of Waste Age at Burial: Slab Calculation.

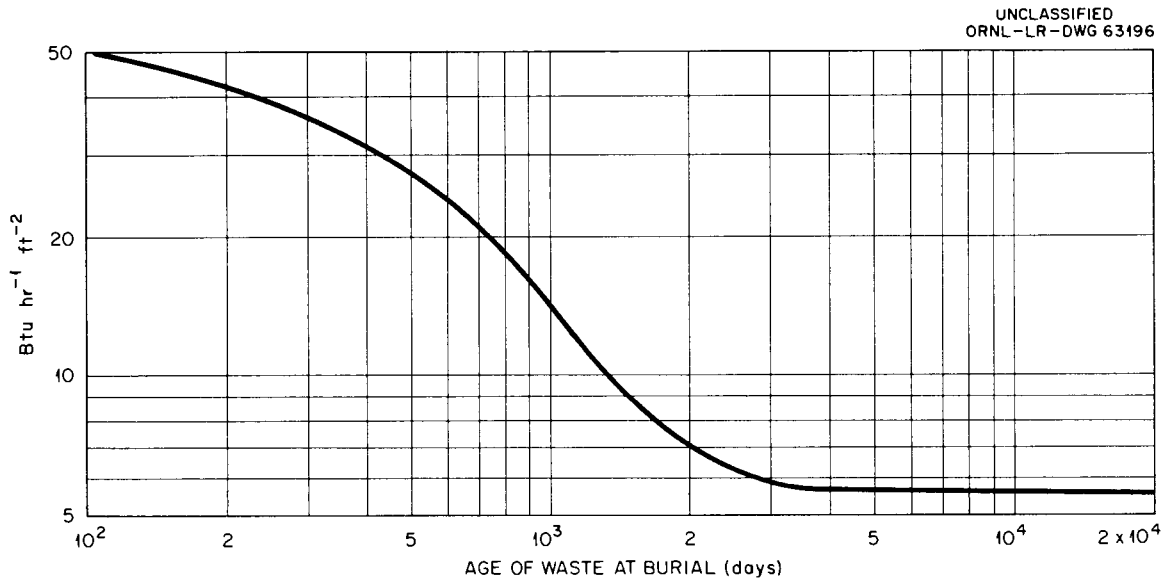


Fig. 4.2. Maximum Allowable Heat Generation Rate for 125°C Peak Salt Temperature Rise: Slab Calculation.

UNCLASSIFIED
ORNL-LR-DWG 63197

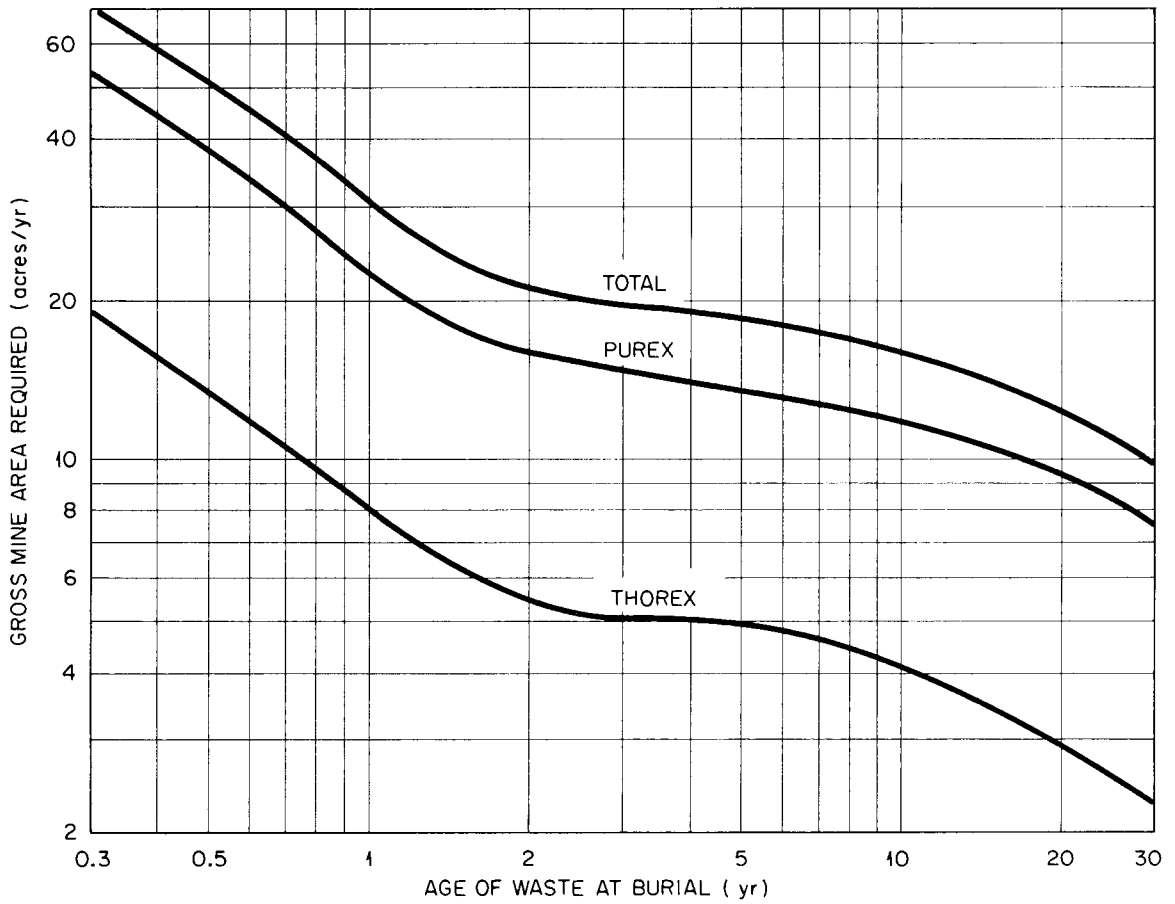


Fig. 4.3. Gross Mine Area Requirements for Liquid Waste Storage. Fifty percent utilization of gross area for waste storage is assumed.

	Minimum Decay Time (years)		
	R = 0.25 ft	R = 0.50 ft	R = 1.0 ft
Acidic Purex	1.7	4.0	19.0
Reacidified Purex	0.61	1.63	3.8
Acidic Thorex	0.45	1.5	3.8
Reacidified Thorex	0.33	0.33	1.15
Acidic Thorex Glass	0.33	-	-

5.0 DISPOSAL IN DEEP WELLS

5.1 Disposal by Hydraulic Fracturing (W. de Laguna)

Test drilling at the experimental site has made slow progress due to interruptions in the work. A hole 100 ft south of the injection well penetrated both grout sheets at depths slightly less than that of the beds into which they were injected and also reached the quartzite at a lesser depth than anticipated. Detailed analysis of these structures will require a survey of the deviation from vertical of the test wells, and arrangements for this survey have been completed.

Mix Subcontract (E. G. Struxness). Westco Research, a subsidiary of The Western Company (Fort Worth), was successful bidder for a Laboratory subcontract to develop a waste-cement-clay mixture to be used in the proposed ORNL Fracturing Disposal Plant. Negotiations were completed and the subcontract was submitted to the Atomic Energy Commission for approval.

The scope of the work to be performed under this subcontract involves the development of a self-solidifying waste mixture to be injected into hydraulically fractured shale and subject to the following controls:

1. The ability to control viscosity during the period of injection, as a low viscosity will reduce the pumping pressures required and a higher viscosity may be needed to keep solids from settling or to control the thickness of the fractures formed.
2. The ability to control the rate of the hardening.
3. The ease of mixing and the possible use of wetting agents.
4. The possible need to use fluid-loss additives.
5. Fluid retention, whether by chemical combination, water of crystallization, or in minute pore spaces in the mix, and the permeability of the mix.

6. The possibility of gelling fluid retained in pores or raising its viscosity by suitable additives, provided the increase in viscosity can be delayed until the injection is completed.
7. Sufficient crushing strength of the solid matrix to support the load of the overburden under well conditions if fluid is to be retained in pores.

The mixture(s) will be tested in temperature and pressure environments simulating well depths of 500, 3000 and 5000 ft in interbedded shale. ORNL will co-operate with Westco in determining the effect of radiation on mixes and their ion exchange properties. The period of performance will be from the date of final subcontract approval to Dec. 31, 1962.

5.2 Liquid Injection into Permeable Formations (D. G. Jacobs)

The disposal of radioactive waste solutions to deep permeable formations provides a means for isolating large volumes of low-activity waste from the circulating regimen of ground water, surface water, and atmospheric water. Several component problem areas require further study before use of this method will be considered.

Movement of Radionuclides in the Disposal Formation. This problem will involve describing the reservoir and its limiting boundaries with regard to the continuity and uniformity of porosity, permeability, pressure gradients, chemical compatibility, and mineralogy. These factors will affect dispersion of the solution front and will impose a limit on the geometrical configuration of the disposed wastes. Dispersion of the solution front, along with chemical interactions of the waste solution, is closely related to the chromatographic distribution of radionuclides in the disposal formation.

Dissipation of Heat. Although it is unlikely that dissipation of heat will be a limiting factor in the disposal of low- and intermediate-level radioactive wastes, it becomes more important when the loading of radionuclides on the sorptive minerals is increased. Thermal conditions can be approximated if the spectra of radionuclides in the waste stream, their geometric distributions in the disposal formation, and the thermal properties of the disposal medium are known.

Protection of the Reservoir Against Plugging or Fracturing. Several factors may contribute to the decreased suitability of an injection well for radioactive waste disposal. If plugging occurs, increased pressure is required to maintain a satisfactory pumping rate, or fracturing may occur and permit rapid breakthrough of activity into pressure-relief wells without adequate contact between the waste solution and the sorptive medium. Plugging may occur because of suspended solids in the waste stream, chemical precipitation reactions between the receiving formation and the injected wastes, corrosion products from injection equipment, growth of microorganisms at the injection face of the formation, or swelling of clays in the formation when the injected waste stream is of lower salt concentration than the solution in the formation.

Corrosion. Corrosion studies may be necessary, depending on the nature of the wastes considered for disposal. Not only will corrosion limit the life of the injection system and auxiliary equipment, but products of corrosion will contribute to reducing the permeability of the receiving formation and will result in increased operating costs.

Injection Equipment Design. Design of the injection system and auxiliary equipment will depend on the type of waste to be disposed of, the activity level of the waste, the volume of waste liquid, and the injection pressures required. Although some limits for design criteria could be established now, more exact requirements will be possible only after other requirements are surveyed.

Health Physics Evaluation. The Health Physics aspects of deep well disposal are twofold. The first involves radiation protection and personnel monitoring of the operating crews. This part of the problem will deal primarily with the external radiation and required shielding for storage and injection of radioactive waste solutions as well as surface contamination problems attendant to the transfer and injection operations. A second aspect is the long-term environmental problem that will occur when the radionuclides reach the pressure-relief wells. Evaluation of this problem will require quantitative definition of the movement of the radionuclides and may require some intermediate observation wells for monitoring, in addition to the constant monitoring of the pressure-relief wells. Extrapolation of data obtained from the intermediate observation wells should be possible if the hydrodynamics and sorptive properties of the formation have been adequately surveyed.

Co-ordination of Effort. In considering any of the component problems, it is possible to overemphasize one particular phase unless a continued effort is made to co-ordinate all phases of the work. In order to co-ordinate the efforts of various co-operating agencies involved in this program, the Reactor Development Division, Washington, AEC has named Prof. W. J. Kaufman (U. of California), chairman, J. Wade Watkins (U. S. Bureau of Mines), and W. de Laguna (ORNL) to serve as an ad hoc advisory committee on programs related to the injection of radioactive liquid wastes into deep permeable formations. The committee first met in August 1961 at Berkeley, California, to discuss the general problem areas and to make recommendations on the role of the various co-operating agencies.

Although ORNL will probably become involved in several phases of the program, initial efforts will be directed primarily to a determination of the expected movement of the radionuclides in the disposal formation. Some work is planned on defining the dispersion of solution fronts, but the primary effort will be concerned with the sorptive properties of cores obtained from typical permeable formations.

Ion exchange processes play an important role in restricting the movement of cationic radionuclides through a geologic formation. However, such a simple picture is not adequate for describing the restricted movement

of many of the radionuclides of concern in low- and intermediate-level waste streams. Strontium has nearly the same exchange potential as calcium on most natural ion exchange materials, and, in systems where there is appreciable calcium, the restriction of strontium movement due to ion exchange is quite low. However, in most formations, minerals are present which form insoluble compounds with strontium and calcium in the waste stream and, when basic conditions are maintained, the waste stream is scavenged of its strontium.

The buffering capacity of a geologic formation, due to the presence of exchangeable hydrogen ions on the clay minerals, is quite high, so that the pH of the injected solution is modified as the solution moves through the receiving formation. Exchange of other stable components of the waste stream also causes considerable modification of the chemistry of the solution as it moves through the formation. These changes have some effect on the ion exchange processes involving radionuclides, but the effect on transition element behavior (e.g. Ru-106) may be much more pronounced, especially when there are changes in oxidation-reduction states. Micaceous minerals in the disposal formation incorporate cesium ions into their crystal lattices in a very slowly reversible process. The exclusion of sodium and calcium ions, the major cationic constituents of most low- and intermediate-level waste streams, is so complete that the total exchange capacity of the formation materials is secondary to the number of lattice fixation sites available when cesium removal is being considered.

Although simple models of ion exchange can be used for approximating the movement of specific radionuclides in a geologic formation, the effect of the formation on the chemistry of the percolating solution must be considered before a comprehensive picture can be developed. Outlined below is the planned method of attack:

1. Obtain representative cores wherever possible.
2. Measure the chemical, physical, and mineralogical properties of the cores.
 - a. Permeability.
 - b. Porosity.
 - c. Acid-base stability.
 - d. Particle size distribution.
 - e. Clay mineralogy.
 - f. Exchange capacity.
 - g. Exchangeable ions.
 - h. pH.
 - i. General mineralogy.
3. Describe the spectrum of waste streams to be considered for disposal.
 - a. Stable ion composition.
 - b. Radionuclide composition.
 - c. Acidity, acid deficiency, or pH.

4. Determine the solution dispersion properties of representative cores as a function of:
 - a. Core length.
 - b. Flow rate.
 - c. Permeability.
5. Determine the sorptive properties of the core materials for various radionuclides from the various types of waste streams, evaluating such parameters as:
 - a. Core length.
 - b. Flow rate.
 - c. Stable ion composition of the waste stream.
 - d. Clay mineralogy.
6. Correlate the breakthrough curves obtained for the various radionuclides with those obtained for dispersion of the solution front.
7. Check the effect of additives to the waste stream on the sorptive properties of the sorbing minerals. (Much of this work has already been done for cesium and strontium and we can make fairly good predictions based on the clay mineralogy of the formation. However, a check is always worth the effort.)
8. Study the possible migration of radionuclides into boundary materials.

6.0 DISPOSAL IN NATURAL SALT FORMATIONS

6.1 Field Tests (F. M. Empson)

Detailed examination of the large field cavities was completed and the cavities were filled. Instrumentation and power supply equipment was placed in standby condition for use in future experiments, and other equipment was packed for return to Oak Ridge or for disposal.

Heat Transfer Array (R. L. Bradshaw and F. M. Empson). The theoretical temperature rise around isolated cylindrical sources was checked against experimental data and found to be in reasonable agreement. Temperature rises in arrays of heat sources can be calculated theoretically by summing the contributions from individual sources; however, several factors make it desirable to have an experimental check with an array containing several heaters. An experiment is planned with a square array containing 16 heaters spaced 3 ft on centers. The heaters will be about 3 ft long and will be located 12 ft below the floor. Power input will be held constant at a rate such that the temperature in the center of the array will reach a value well over 100°C.

Figure 6.1 is a plan of the array being prepared in the mine at Hutchinson. Thermocouple holes within the array will be 15 ft deep except for the center hole which, along with those outside the heater array, will be 30 ft deep. Approximately 30 holes have been drilled.

Salt Permeability (F. M. Empson). Three horizontal holes, 3 in. dia, were drilled into the wall at the Lyons mine. One hole extends to the center of a

square column ~40 ft on each side and is located in the essentially shale-free salt 3.5 ft above the floor. Two are drilled 30 ft into a perimeter wall of the mine. One is located in a "black line" of high-shale-content salt about 5 ft above the floor, and the other is in salt relatively free of shale, just above the "black line." These holes are to be used for a test, under field conditions, of the permeability of the salt structure to gases by using a packer to seal the hole and helium or nitrogen as the test gas.

Low-Level Packaged Solids Disposal in Salt Formations (F. M. Empson). The objective of low-level solid radioactive waste disposal is to isolate the waste in such a way that contact with ground or surface water is minimized. These criteria are met by the large amount of space created in salt formations by mining operations. A disposal operation in mined space in salt would have the additional advantage that monitoring and isolation of the site would not be required after filling of the mine.

Open mine space exists in Western New York, at Detroit, Mich., in Central Kansas, in Louisiana, and in Texas. The New York and Michigan sites are more favorably located for the Northeast, where the bulk of these wastes originate, and the other sites are as convenient as the present sites at Oak Ridge and Idaho Falls. A study is in progress to evaluate transportation and long-term monitoring costs as they affect the economics of low-level waste disposal by surface burial and in mined space underground.

6.2 Plastic Flow Studies (W. J. Boegly, Jr.)

In September 1959, five Extensometers were installed in a recently mined-out area in the Hutchinson mine by representatives of the Department of Civil Engineering, University of Texas, as part of their Reactor Fuel Waste Disposal Project (7). The purpose of these gages was to obtain information on the creep of rock salt. A recently mined-out room was used since the flow rates (creep) would be high and the data could be extrapolated to estimate the flow rates just after the opening was created. Of the five gages (Fig. 6.2), four were installed to measure deformation between the floor and the ceiling, and one was installed to measure deformation between the side walls of the room.

Analysis of the measurements taken to date indicates that the rate of deformation decreases with time and, further, that an exponential equation can be derived to describe the relation between rate of floor movement ($\mu\text{in./in./day}$) and time (days) since the opening was mined, or, if desired, the time since the gages were installed. The result of statistical curve fitting for data from each gage is given in Table 6.1, and a typical plot of the data from one gage is shown in Fig. 6.3. The maximum closure predicted by integrating these equations from $t = 0$ to $t = \infty$ and the time for 95% of maximum closure are also included in Table 6.1. It is of interest to note that there does not appear to be a significant difference between the flow rates observed for any of the gages at any given time. This means, at least during the period under investigation, that there is no significant difference between the rate of movement near the center of the room and near the columns. This does not agree with measurements from the gages located in the older room (30-year opening) in which the experimental waste cavities are located (2), and may be due to the differences in age of the mined openings.

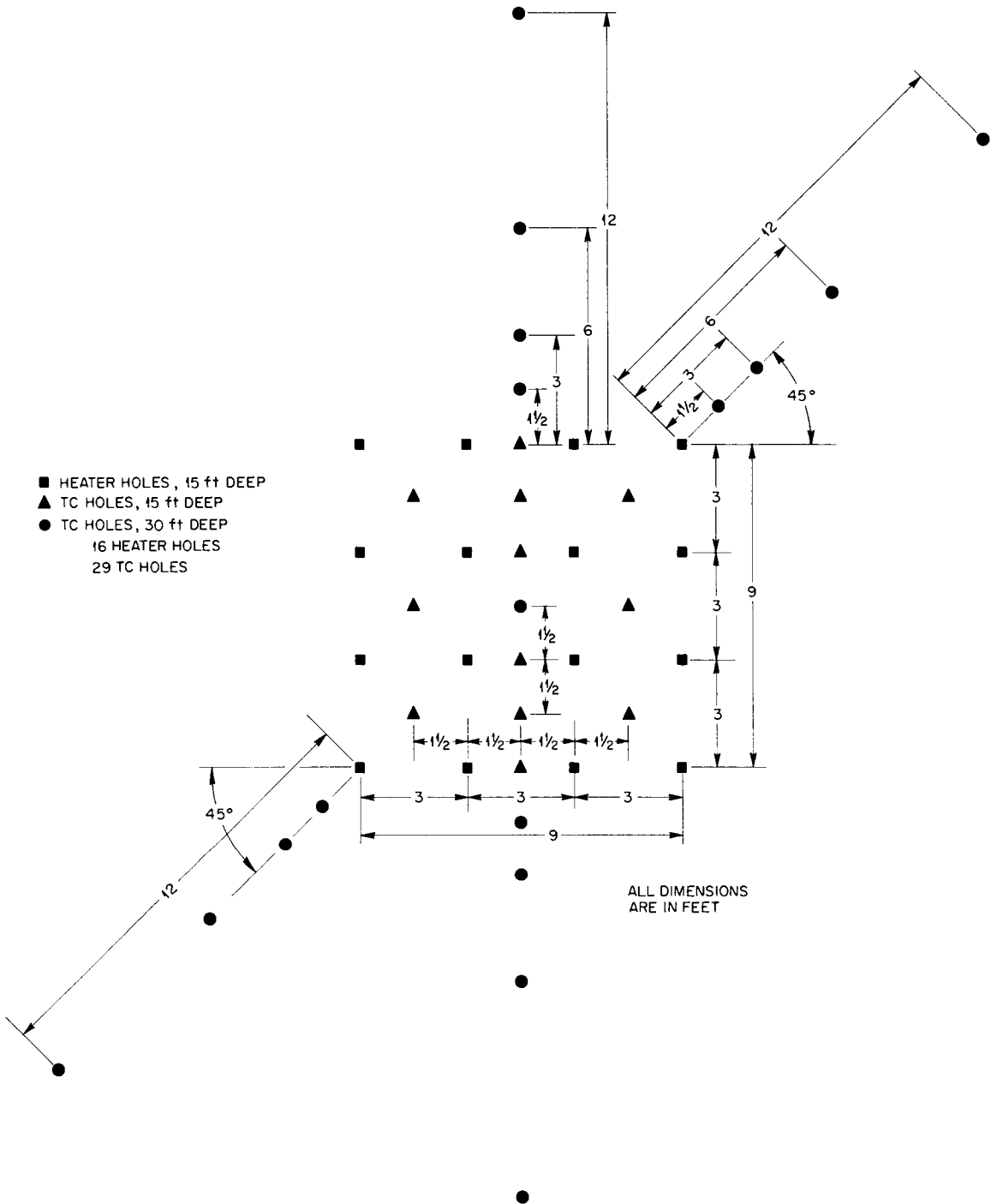


Fig. 6.1. Heat Transfer Array To Check Temperatures Resulting from Many Heat Sources.

UNCLASSIFIED
ORNL-LR-DWG 63199

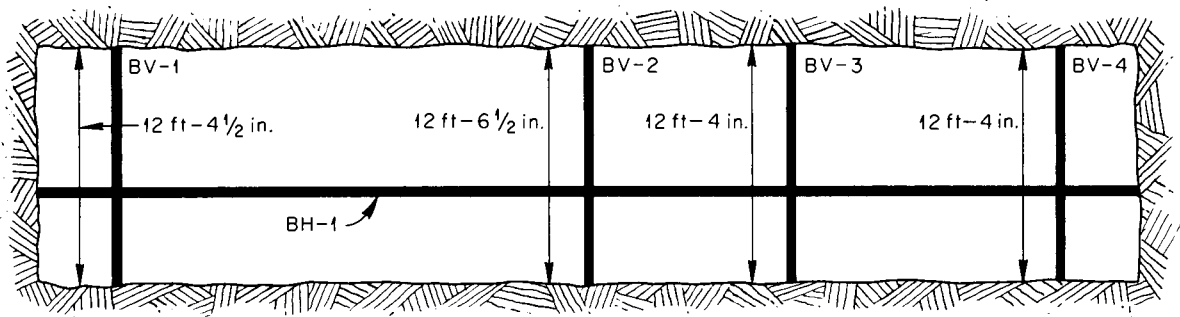
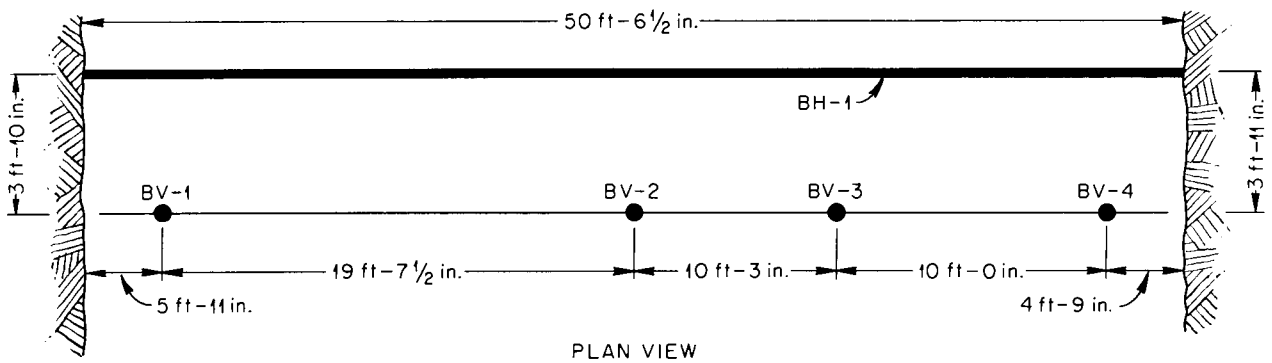


Fig. 6.2. Room Mined in January 1959.

UNCLASSIFIED
ORNL-LR-DWG 63200

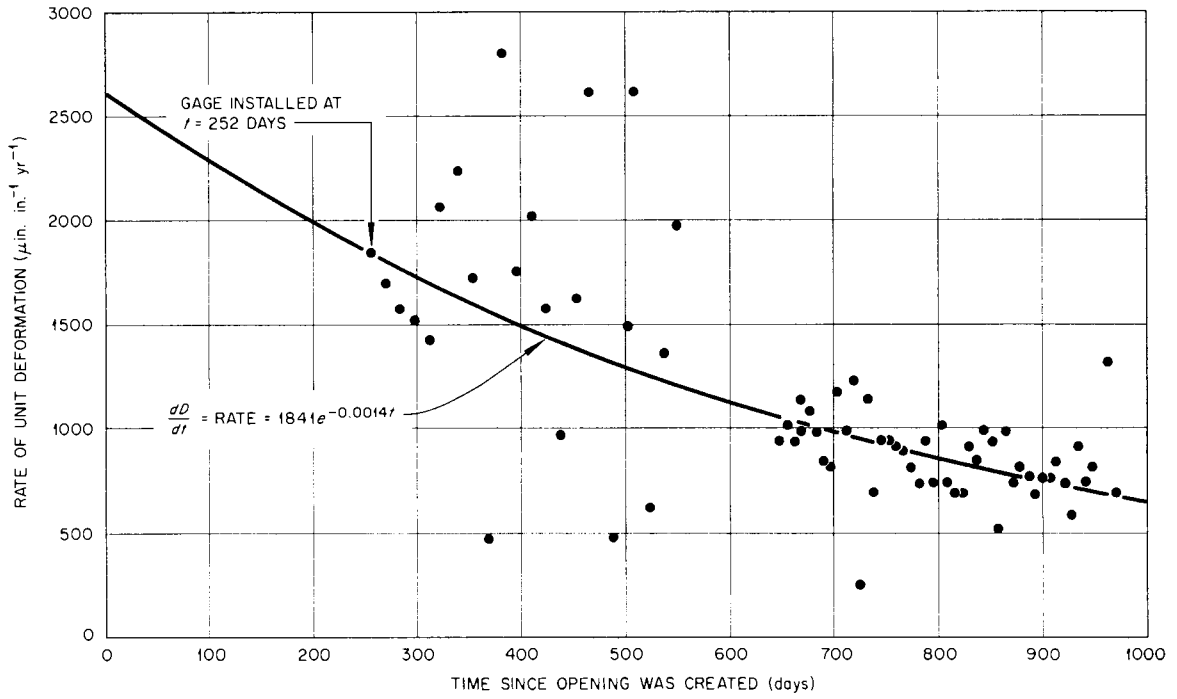


Fig. 6.3. Rate of Unit Deformation vs Time for Extensometer Gage BV-1.

Table 6.1. Flow Equations for Newly Mined Room in the Carey Mine, Hutchinson, Kansas

Gage	Rate of Unit* Deformation ($\mu\text{in./in./yr}$)	Total Movement* ($\mu\text{in./in.}$)	Max Closure (%)	Time of 95% of Total Closure (years)
BV-1	$\frac{dD}{dt} = 1841 e^{-0.00140t}$	$D = 5.044 \int e^{-0.00140t} dt$	0.36	5.86
BV-2	$\frac{dD}{dt} = 2107 e^{-0.00147t}$	$D = 5.773 \int e^{-0.00147t} dt$	0.39	5.58
BV-3	$\frac{dD}{dt} = 2099 e^{-0.00150t}$	$D = 5.751 \int e^{-0.00150t} dt$	0.38	5.47
BV-4	$\frac{dD}{dt} = 2062 e^{-0.00146t}$	$D = 5.649 \int e^{-0.00146t} dt$	0.39	5.72

*t is time in days.

Projection of the equations in Table 6.1 to a point at which t is equal to 10,000 days (~ 30 years) indicates flow rates considerably smaller than those observed in the room containing the experimental cavities. Thus, mining of the cavities upset the equilibrium of the room and initiated flow in excess of what would normally have occurred. It is not possible to verify this since the gages were not installed until the cavities had been excavated; however, it may be possible to install gages in a similar size room adjacent to the room containing the experimental cavities for measurements of flow now occurring in the salt.

Preliminary attempts to use the same type of equations for flow data around the waste cavities indicated that the nature of the flow is not the same as observed in the active area of the mine. For the period prior to heating, flow seems to occur with a constant rate, and not at a rate decreasing with time. This further substantiates the belief that excavation of the cavities had a very significant effect on salt flow in the room containing the experiments.

Three gages were installed in the Lyons, Kans., mine of the Carey Salt Company to measure flow in a mine at greater depth and with greater percentage salt extraction. One of these gages is located in the last room mined prior to termination of the mining operation, in a room which shows no visual evidence of floor "buckling" or ceiling "sag." The purpose of this gage is to obtain information on flow at greater depths and also as background information on the possible use of this area for tests with high-activity solids. The other gages are located in an older section of the mine to measure flow in the floor and ceiling of rooms of the same dimensions. The basic difference between these gage installations is that the first is attached between the salt roof and the salt floor, whereas the ends of the second gage are installed in shale located

about 1 ft above the salt ceiling and in the shale about 1 ft below the salt floor. It is hoped that data will be obtained to show that relatively thin layers of salt above the roof and below the floor are moving, or being squeezed, at a faster rate than the overlying shale. This assumption is based on observations in other areas of the mine in which the upper 1 ft of salt above the ceiling of the room has "sagged" and the relatively thin layer of the salt above the shale parting in the floor has "buckled" due to the pressure transmitted to the salt by the pillars. Not enough measurements have yet been made to predict the rate of movement or expected maximum closure of these rooms, but the few measurements made thus far indicate that the amount and rate of deformation are much less than those observed in Hutchinson; however, it is a much older mine and the flow would be expected to be very small.

6.3 Thermal Studies (R. L. Bradshaw)

Cylindrical Heat Sources. The slab calculation (2) gives a conservative estimate of space requirements for an evenly distributed heat source, but if discrete sources are used, it is necessary to correct for the temperature perturbations around the sources.

Since the cylinder is a likely storage container geometry for solid wastes it is desirable to have a solution for temperature rises about cylindrical heat sources. An equation is available for an isolated line source of constant heat-generation rate, and if a cylindrical source is long compared to its diameter, this gives a good approximation of the temperature rises in the medium surrounding the cylinder (other methods are available for obtaining the temperature profile within the cylinder itself). This equation requires numerical integration and produces only the results for a steady heat-generation rate; however, the varying-heat-source solution could be programmed in a manner similar to that used for the infinite slab. R. E. Glover of Denver, Colorado, a consultant, using the isolated line source equation, manually calculated the time-temperature profile on a line perpendicular to the center of the constant heat source at distances from the center of 1/24, 0.5, 1.0, 1.5, 2.0, and 3.0 times the length of the source, which are shown in Fig. 6.4 along with curves for additional values of x/L obtained from a cross-plot.

Two tests were run in the Carey mine using Calrod-type heaters to obtain data on the time-space temperature profiles near an isolated cylindrical heat source. One heater was located in the center of the floor of a corridor and the other half-way up the wall of a pillar. Each heater was placed in a sand-filled iron pipe. This assembly was then placed in a 1-3/4-in.-dia hole and the hole back-filled with sand. The heaters had an active heating length of 6 ft and were located with their centers 10 ft below the salt surface. Thermocouples were inserted in polyethylene tubing and placed in 1-3/4-in. holes backfilled with sand.

Figure 6.5 shows the temperature rises obtained at distances of 2, 4, 8, and 16 ft on lines perpendicular to the centers of the heaters with power input held constant at 2000 watts. The points shown were obtained in three

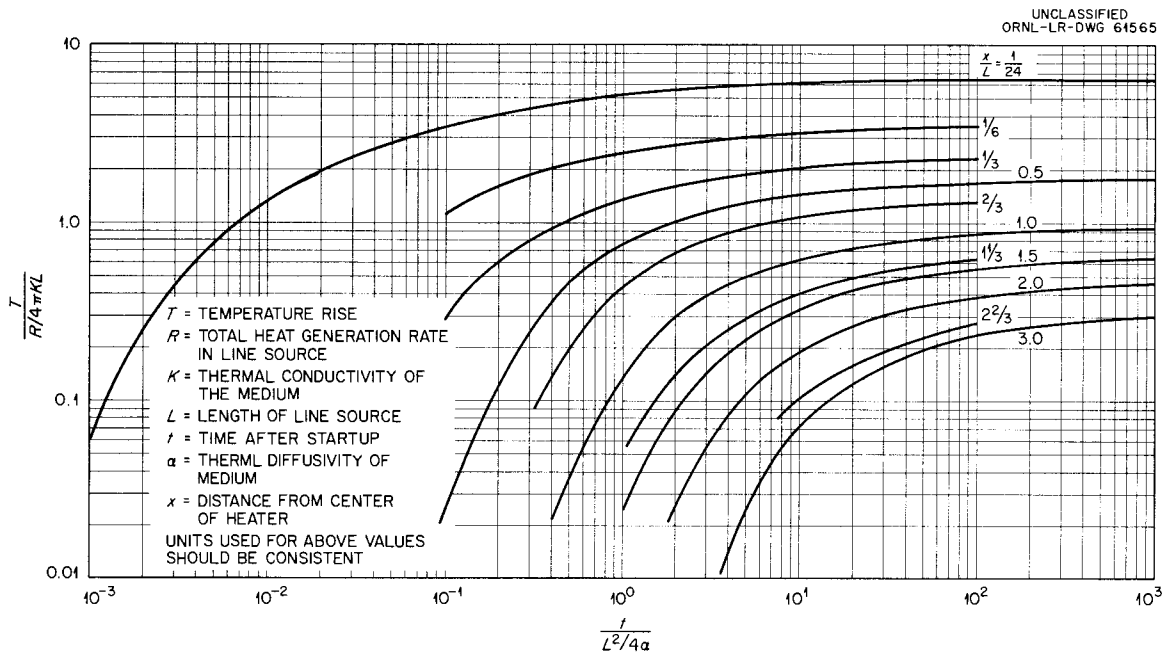


Fig. 6.4. Temperature Rise Around a Line Source with a Constant Heat Generation Rate.

UNCLASSIFIED
ORNL-LR-DWG 63204

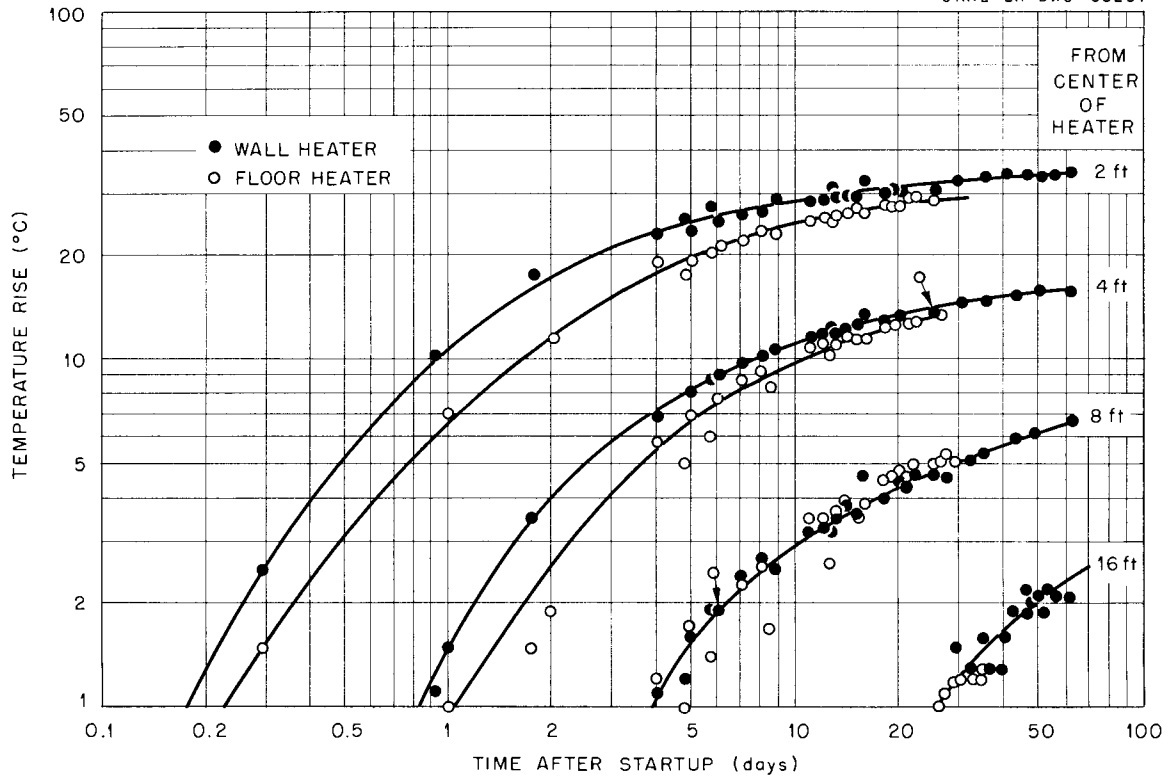


Fig. 6.5. Temperature Rise Around 6-ft Rod Heaters in Wall and Floor of Salt Mine. Heat generation rate ~ 2000 watts.

different runs, with the salt allowed to return to ambient temperature between runs. Although pillar and floor test results do not agree exactly, there appears to be no great difference in the heat-transfer capabilities of the two locations, even though there are considerable shale and anhydrite in the floor while the pillar is nearly pure salt. The measured temperature rises agree reasonably well with the theoretical curves of Fig. 6.4. The scatter in the experimental data does not permit accurate determination of the thermal properties of salt, but the conductivity appears to be approximately $3.0 \text{ Btu hr}^{-1} \text{ ft}^{-1} \text{ }^{\circ}\text{F}^{-1}$ and the diffusivity $0.10 \text{ ft}^2/\text{hr}$.

An equation for the temperature distribution about a finite-length cylinder located in an infinite array of cylinders was developed (reference 2, Sect. 4.0) in connection with the economic study of disposal in salt. The status of the computer program for computation is discussed in Sect. 4.0 of the present report.

Thermal Properties of Salt. Birch and Clark measured the temperature dependence of conductivity and diffusivity of single natural Halite (NaCl) crystals (8) (Fig. 6.6). Preliminary measurements made by the U. S. Geological Survey with granular salt compacted under high pressure are in substantial agreement with those of Birch and Clark for the single-crystals (9).

The conductivity and diffusivity values obtained in the field tests with cylindrical sources (preceding section) and with the 7.5-ft cubes (Sect. 6.3 of reference 2) are only 10 - 20% lower than those for the single crystal (Fig. 6.6). In addition, laboratory tests at 28°C of both irradiated and unirradiated aggregate samples indicated approximately 25% lower conductivity than that of the single crystal (10). This relatively close agreement lends confidence to theoretical calculations of temperature rise based on single-crystal values. Both the conductivity and diffusivity (Fig. 6.6) decrease rather sharply with increasing temperatures, while the theoretical equations developed to date assume constant thermal properties. To be conservative, theoretical calculations must be made with values for the thermal properties at the highest temperatures that may be reached in a particular case. It has been felt that this may impose an unduly severe restriction since only the salt in contact with the waste or waste container will ever reach this peak temperature, while salt at greater distances may be at much lower temperatures. The most recent results obtained with the infinite-slab equation (2) indicate that this need not be a concern, at least for the slab geometry, since the peak temperature rise is not a strong function of conductivity and diffusivity. For example, the peak temperature rise in the slab calculated with the 100°C salt conductivity and diffusivity was only 18% less than that calculated with the 300°C salt thermal properties, even though the conductivity was 70% greater and the diffusivity 90% greater than at 300°C .

It has been found that unrestrained rock salt aggregates shatter rather violently when heated in a muffle furnace to temperatures of $250 - 300^{\circ}\text{C}$. (It is speculated that this may be due to the presence of small quantities of water trapped in negative crystals or to oxidation of organic impurities.) If this shattering occurs in salt in situ it may result in poorer thermal

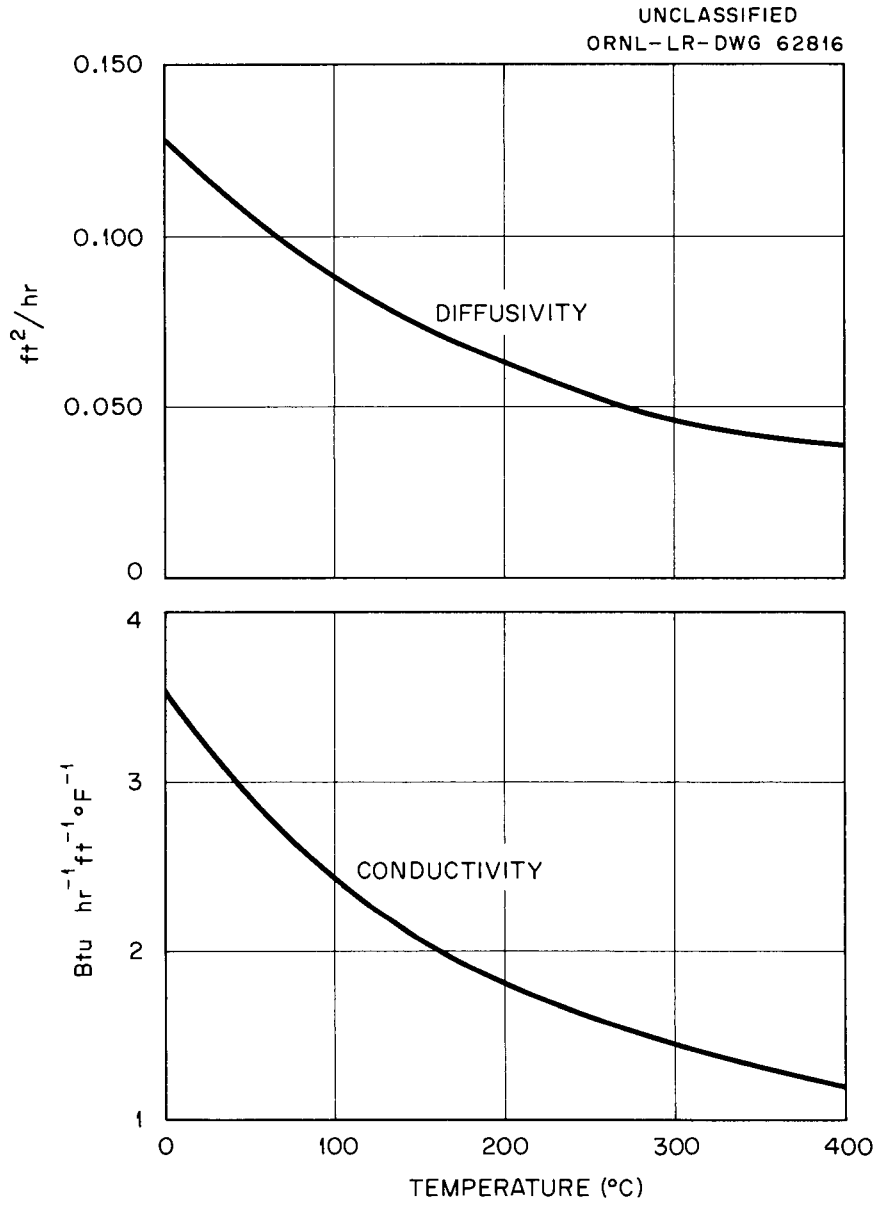


Fig. 6.6. Thermal Properties of Halite (Adapted from Birch and Clark).

conductivity and consequent increased waste temperature rise. Since this effect may place an upper limit to the allowable salt temperature rise, both laboratory and field tests are planned to investigate it.

7.0 CLINCH RIVER STUDY

7.1 Estimate of Activity in Bottom Sediments (P. H. Carrigan*)

In connection with the investigation of distribution of radioactivity in bottom sediments of the Clinch River the variation in sediment size in the Study Reach (CRM 4.1 to CRM 20.8) was studied. Studies of the longitudinal distribution of radioactivity indicated that the maximum activity is associated with sediments deposited midway in the reach.

Core samples of the bottom sediments were collected at 10 equally spaced intervals along four cross-sections previously monumented by TVA, CRM 4.7, 7.6, 11.9 and 19.2, and at another cross-section, CRM 15.3. The cores for each cross-section were composited. The composites were submitted to the North Carolina District, Quality of Water Branch, U. S. Geological Survey, for size distribution analyses. The results (Table 7.1) indicate that the size of sediment is generally < 1 mm. The average clay content is about 14 wt %, and the sand content varies from 30% at the lowest cross-section to 40% at the uppermost cross-section. According to the U. S. Bureau of Soils classification, the sediments vary in texture from silty loam to loam. The distribution of sizes would be classed as well graded clay to the upper range of sand sizes. The average median diameter is 28μ (0.028 mm), and the maximum median diameter (39μ) is at the uppermost cross-section and the minimum (20μ) at CRM 11.9. At CRM 4.7 the median size is 25μ . Results of the study of size distribution will be correlated with other physico-chemical properties that may affect the distribution of radioactivity in the reach. The data will be applied, also, in studies of the probable magnitude of bottom sediment (bed load) movement.

7.2 Dispersion Study

On Aug. 30, 1961, 7.5 curies of Au-198 was dispersed over the full width of the mouth of White Oak Creek in 67 sec. The concentration at this point was about 9400 times the MPC_w. At the time of release of the radioactive tracer the flow from White Oak Creek was about 7 cfs, the flow in Clinch River had been steady since Aug. 28 at 8000 cfs, and the level of Watts Bar Reservoir was between 740 and 741 ft above mean sea level. Under these conditions of flow and method of injection the development of dispersion, travel time, and reduction in concentration in the study reach of the Clinch River were to be studied.

The mouth of White Oak Creek is on the right bank of Clinch River at CRM 20.8, and immediately downstream is Jones Island (CRM 20.6). The tracer released in White Oak Creek remained concentrated near the right bank of the Clinch in the vicinity of Jones Island. At CRM 19.6 the activity had spread from bank to bank, but was not uniformly dispersed. Activity had become uniformly dispersed in the width and depth of cross section at CRM 17.1, 3.7 miles downstream from the mouth of White Oak Creek.

*On loan from Tenn. District Surface Water Branch, Water Resources Division, U.S. Geological Survey.

Table 7.1. Size Analysis of Clinch River Bottom Sediments

CR Mile	Sp. Gr.	Percent Finer than Indicated Size									
		0.002 mm	0.004 mm	0.008 mm	0.016 mm	0.031 mm	0.062 mm	0.125 mm	0.250 mm	0.500 mm	1.000 mm
4.7	2.73	12	15	26	39	55	70	82	91	94	96
7.6	2.64	13	18	28	42	58	67	87	96	99	100
11.9	2.58	14	19	31	45	60	69	89	98	100	--
15.3	2.66	16	21	28	40	50	62	74	92	100	--
19.2	2.49	12	17	22	32	45	60	78	93	99	100

Because of lateral, vertical, and longitudinal dispersion the peak concentration of Au-198 in Clinch River water was decreased by a factor of 500 from CRM 20.8 to CRM 17.1. Downstream from CRM 17.1 dispersion was largely longitudinal, and therefore there was a much smaller reduction factor in peak concentration. From CRM 17.1 to CRM 4.5 (Centers Ferry) Au-198 concentration was decreased by a factor of < 10 .

Travel time from the mouth of White Oak Creek to Gallaher Bridge, CRM 14.5, at the intake to the water plant of ORGDP, was 7.9 hr. The concentration of Au-198 at this cross-section was 8% MPC_w. From the point of release to Centers Ferry, CRM 4.5, the travel time was 30.2 hr and the concentration was 3% MPC_w.

7.3 Error in Estimate of Sediment Activity

The rate of change of activity with distance (curies/mile) and total activity (curies) reported previously (1) were computed incorrectly. Specific activity, listed in $\mu\text{c}/\text{kg}$, was determined for dry weight of solids in the bottom sediments. The mass of bottom sediments, in g/mile, was computed for wet weight of sample. The correction factors are not constant because of the variability of water content of the composite samples and of specific gravity. The total activity was recomputed on the basis of dry weight of solids for the reach CRM 4.7 to 21.6, as 13.2, 43.2, 4.71, 0.700, and 14.7 curies, respectively, for Ru-106, Cs-137, Co-60, Sr-90, and total rare earths.

8.0 FUNDAMENTAL STUDIES OF MINERALS

8.1 Considerations in Cesium Selectivity (T. Tamura)

Selectivity of clays for cesium was shown to be related to the collapsed-lattice minerals such as the potassium-bearing illite and micas. Since sodium-fluorophlogopite (a synthetic mica) was more selective for cesium than the potassium-fluorophlogopite, it was reasoned that the beneficial role of potassium in minerals was to maintain the collapsed lattice.

To demonstrate the effect of the collapsed lattice, vermiculite was treated with potassium chloride solutions and the lattice (c-spacing) collapsed from 14 to 10 Å. The resultant K-vermiculite was more selective for cesium in spite of a decrease in exchange capacity from 65 to 17 meq/100 g. Later studies of biotite micas showed improved cesium removal if the exchange capacity of mica was increased. These studies emphasize the importance of two variables: exchange capacity and structure. The most desirable combination in a mineral would be a lattice partially collapsed for favorable cesium selectivity but partially open to retain the maximum exchange capacity of the mineral.

The possibility of attaining the desired conditions was suggested by some data on vermiculite saturation reported by Walker (11), viz., that barium and lithium ions decrease the spacing of vermiculite from 14 to 12 Å. This spacing may be compared with 14 Å reported for magnesium and calcium saturation and 10 Å for potassium and ammonium saturation.

Cesium Selectivity of Vermiculite with Different Ion Saturation. Samples of vermiculite saturated with barium and lithium had 12 Å spacing, but only Ba-vermiculite showed a significant increase in cesium selectivity (Table 8.1a). It is important, perhaps, to note that barium is close to cesium in ionic radius (1.35 vs 1.69 Å) but the lithium ion is much smaller (0.60 Å). Al-vermiculite showed the lowest selectivity, possibly because of the open lattice of the mineral when saturated with aluminum and the trivalent nature of aluminum. The K-vermiculite response was similar to earlier findings.

The samples of vermiculite were saturated with different cations by treating known weights of vermiculite with ~10 times the exchange capacity in solutions containing the approximate chloride salt of the cation. Excess salt was then washed from the mineral by distilled water until AgNO₃ tests of the wash were negative, and the samples were then air-dried. To calculate the weight of each form of vermiculite equal to 1 g on an oven-dried weight basis, a separate aliquot was heated to 105°C overnight and the weight loss determined. The samples were slurried in 20 ml of 1.5 M NaNO₃ solution containing 25 mg Cs/liter.

Cesium Selectivity of Montmorillonite with Different Ion Saturation. Although vermiculite is easily collapsed by simple chemical treatment, montmorillonite does not collapse to 10 Å by such treatment but potassium saturation has been shown to decrease the c-axis spacing of montmorillonite from 14 to 12 Å (compared to 10 Å in vermiculite). In tests with montmorillonite, K-montmorillonite showed an increase in cesium sorption, but Ba-montmorillonite did not. X-ray diffraction diagrams showed a c-spacing of 14 Å for the alkaline earth cations. As with Al-vermiculite, Al-montmorillonite showed the lowest selectivity for cesium. Apparently, with the montmorillonites equilibrium is established rapidly. The slow equilibrium reaction of vermiculite may be due to large particles and the presence of biotite impurities. The biotite structure prevents easy access to exchange sites and thus decreases the rate of the equilibrium reaction.

The montmorillonite was saturated with the different cations similarly to the vermiculite saturation described above and was slurried with 1.5 M NaNO₃ solution containing 25 mg Cs/liter.

Exchange Capacity. For better characterization of materials used in these experiments, the ion exchange capacities of samples saturated with different cations were measured. As expected, potassium treatment decreased the exchange capacity of vermiculite (Table 8.2), as a result of collapse of the lattice to 10 Å, and the fixed K was not replaced during saturation with CaCl₂. The exchange capacity measurements of Ba-vermiculite and K-montmorillonite did not show the fixation reaction for these systems.

The experiments were made by saturating the material with Ca, leaching the calcium with sodium acetate, and titrating it with versene. The montmorillonite data suggest that the alkali ions are more difficult to replace with calcium than the divalent ions, the difference probably being caused by the ability of divalent ions to affect the exchange capacity measurements by complexing with versene.

Table 8.1. Percentage Removal of Cesium by Vermiculite and Montmorillonite Saturated with Various Cations

20 ml of 1.5 M NaNO_3 containing 25 mg Cs/liter contacted with 1 g equiv of material

Contact Time (hr)	Cs Removal (%)							
	Natural	K	Na	Li	Ca	Al	Ba	Mg
a. Vermiculite								
1	11.0	12.0	9.59	11.4	9.09	7.66	10.7	--
4	13.4	16.2	13.3	14.7	14.9	16.4	23.6	--
24.5	15.2	19.3	15.3	14.7	15.9	17.5	32.1	--
77	14.6	18.0	15.2	13.4	17.9	14.0	38.0	--
190	16.0	20.6	16.9	15.1	20.0	12.5	43.2	--
b. Montmorillonite								
1	32.7	50.3	25.1	25.5	26.0	20.4	23.1	23.8
4	30.9	49.9	26.4	25.2	27.4	20.9	24.6	23.6
24	31.7	49.1	25.6	25.6	26.6	21.7	25.6	23.6
76	30.8	48.6	25.6	24.9	27.3	21.3	27.5	24.6
144	30.6	48.3	25.5	25.5	26.8	20.7	26.0	24.0

Table 8.2. Ion Exchange Capacity of Vermiculite and Montmorillonite after Saturation with Different Cations

Exchange Agent	Saturating Cation	Capacity (meq/100 g)
Vermiculite	Natural	65.0
	Ba	62.5
	Ca	63.7
	Li	66.5
	K	16.7
Montmorillonite	Natural	91.4
	Ba	84.6
	Ca	85.1
	Li	72.0
	K	78.0
	Mg	86.9
	Na	75.3
	Al	82.2

9.0 WHITE OAK CREEK BASIN STUDY*

T. Lomenick

The rate of ground water movement in the bed of former White Oak Lake was measured by the auger hole method, i.e., by augering a cavity below the water table, allowing it to fill with water, pumping the water level down in the hole, and observing the rate of rise. The rate of rise can be reduced to standard permeability units by a suitable formula (12). Data from two sites in the upper part of the lake bed showed permeability values of 0.5 and 2.6 ft/day, while values from four sites in the lower bed varied from 0.2 to 2.2 ft/day. All cavities were 4 in. dia and 5-6 ft deep. The auger hole method measures essentially the horizontal permeability, but additional field tests are planned to determine the vertical permeability of the lake bed soil.

The alluvial material underlying the bed of former White Oak Lake consists of a complex mixture of sand, silt, clay, and gravel. Core and auger samples taken along transects at the upper, middle, and lower parts of the lake showed that, with the exception of the recent lacustrine deposit, there are no beds that persist vertically or horizontally. However, it appears that the amount of sand and gravel increases with depth while silt and clay decrease. The results of a detailed mechanical analysis of a core sample taken in the upper part of the lake bed is shown in Table 9.1.

Table 9.1 Distribution of Particle Sizes in Core Sample Taken in Upper Part of White Oak Lake

Depth (in.)	Percentage			
	> 2 mm	0.05-2 mm	0.2-50 μ	< 0.2 μ
0-3	0	17.0	54.1	28.9
3-6	0	29.5	51.1	19.4
6-9	0.2	25.4	55.2	19.2
9-12	0.3	28.8	53.0	18.4
12-18	0.6	14.9	59.7	24.8
18-25	0.1	23.2	56.0	20.7
25-33	0	31.6	47.0	21.4
33-39	1.4	27.3	51.0	20.3
39-49	2.5	41.3	35.6	20.6
49-50	0	62.4	18.8	18.8
50-59	31.6	44.6	12.6	11.2
59-66	1.4	49.9	23.8	24.9
66-70	17.9	45.7	22.2	14.2
70-75	18.2	51.3	16.7	13.8

*This project, entitled "Environmental Radiation Studies: Evaluation of Fission Product Distribution and Movement in White Oak Creek Drainage Basin" (AEC Activity Number 060501000) is supported by the U.S. Atomic Energy Commission's Division of Biology and Medicine. All other projects covered in this Bimonthly Progress Report are supported by the Division of Reactor Development (AEC Activity Number 040405021).

10.0. REFERENCES

1. "Waste Treatment and Disposal Progress Report for April and May 1961," ORNL-CF-61-7-3.
2. Ibid. for April and May 1961, ORNL-TM-15.
3. J. M. Holmes, "Waste Calciner Pilot Plant Proposal," ORNL-CF-60-12-121 (Dec 14, 196).
4. J. T. Roberts and R. R. Holcomb, "A Phenolic Resin Ion-Exchange Process for Decontaminating Low-Radioactivity-Level Process Water Wastes, ORNL-3036 (May 22, 1961).
5. R. R. Holcomb and J. T. Roberts, "Low-Level Waste Treatment by Ion-Exchange. II. Use of a Weak Acid, Carboxylic-Phenolic Ion-Exchange Resin," ORNL-TM-5 (Sept. 25, 1961).
6. Dorr-Oliver, Inc., Stamford, Conn., "Informational Report," AEC Research and Development Contract No. AT-(40-1)2246, Jan. 5, 1961.
7. T. D. Reynolds and E. F. Gloyna, "Reactor Fuel Waste Disposal Project: Permeability of Rock Salt and Creep of Underground Salt Cavities," Univ. of Texas, AEC Contract AT-(11-1)-490, Dec. 30, 1960, p. 92.
8. F. Birch and H. Clark, "The Thermal Conductivity of Rocks and Its Dependence on Temperature and Composition," Am. J. Sci., 238: 552 (1940).
9. E. C. Robertson, USGS, Silver Springs, Md., letter of July 10, 1961.
10. F. Birch, Harvard Univ., letter to F. L. Parker, June 6, 1959.
11. G. W. Brindley, "X-ray Identification and Structure of the Clay Minerals," Mineralogical Society of Great Britain Monograph, London, 1951.
12. Transactions, Am. Geophysical Union, 32(4): 582-590 (August 1951).



INTERNAL DISTRIBUTION

1. ORNL - Y-12 Technical Library
Document Reference Section
- 2-4. Central Research Library
- 5-14. Laboratory Records Department
15. Laboratory Records, ORNL R.C.
- 16-17. R. E. Blanco
18. J. O. Blomeke
19. W. J. Boegly, Jr.
20. R. L. Bradshaw
21. J. C. Bresee
22. F. N. Browder
23. K. B. Brown
24. P. H. Carrigan
25. W. E. Clark
26. K. E. Cowser
27. F. L. Culler
28. W. de Laguna
29. F. M. Empson
30. D. E. Ferguson
31. H. W. Godbee
32. H. E. Goeller
33. J. M. Googin
34. C. W. Hancher
35. R. F. Hibbs
36. R. R. Holcomb
37. J. M. Holmes
38. D. G. Jacobs
39. W. H. Jordan
40. H. Kubota
41. T. F. Lomenick
42. K. Z. Morgan
43. R. J. Morton
44. E. L. Nicholson
45. F. L. Parker
46. J. J. Perona
47. R. M. Richardson
48. J. T. Roberts
- 49-50. E. G. Struxness
51. J. C. Suddath
52. J. A. Swartout
53. T. Tamura
54. J. W. Ullmann
55. M. E. Whatley

EXTERNAL DISTRIBUTION

56. E. L. Anderson, AEC, Washington
57. W. G. Belter, AEC, Washington
58. W. H. Regan AEC, Washington
59. J. A. Buckham, Phillips Petroleum Company
60. H. J. Carey, Jr., Carey Salt Company, Hutchinson, Kansas
61. C. W. Christianson, Los Alamos Scientific Laboratory
62. V. R. Cooper, AEC, Washington
63. E. F. Gloyna, University of Texas, Austin
64. L. P. Hatch, Brookhaven National Laboratory
65. W. B. Heroy, Sr., Geotechnical Corp., Dallas, Texas
66. H. H. Hess, Chairman, Earth Science Division, Commission on
Ground Disposal of Radioactive Waste, Princeton University,
Princeton, New Jersey
67. J. R. Horan, AEC, Idaho
68. J. H. Horton, Stanford Research Institute
69. J. F. Honstead, Hanford
70. E. R. Irish, Hanford
71. A. A. Jonke, Argonne National Laboratory
72. K. K. Kennedy, Phillips Petroleum Company
73. W. J. Kaufman, University of California, Berkeley
74. S. Lawroski, Argonne National Laboratory
75. B. M. Legler, Phillips Petroleum Company
76. J. A. Lieberman, AEC, Washington
77. J. A. McBride, Phillips Petroleum Company
78. J. W. Morris, Du Pont, Savannah River
79. R. L. Nace, Water Resources Division, USGS, Washington,
NAS-NRC

80. C. M. Patterson, Du Pont, Savannah River
81. W. H. Reas, Hanford
82. C. S. Shoup, AEC, ORO
83. L. Silverman, Harvard Graduate School of Public Health
84. J. I. Stevens, Phillips Petroleum Company
85. C. M. Slansky, Phillips Petroleum Company
86. V. R. Thayer, Du Pont, Wilmington
87. J. Vanderryn, AEC, ORO
88. Abel Wolman, Chairman, National Academy of Sciences,
Committee on Waste Disposal, Johns Hopkins
- 89-104. Division of Technical Information Extension
105. H. M. Roth, ORO